

Cite this: *Nanoscale Adv.*, 2024, 6,  
5258

# Photocatalytic nanomaterials and their implications towards biomass conversion for renewable chemical and fuel production†

Shikha Katre, Pawan Baghmare and Ardhendu S. Giri \*

Photocatalytic processes have recently gained popularity as a sustainable and energy-efficient method for converting biomass. This article gives a comprehensive overview of recent improvements in the photocatalytic conversion of biomass into useful chemicals and fuels utilizing various photocatalytic materials. The work delves into the assessment of diverse biomass sources and their preparation techniques, in addition to the synthesis of plasmonic nanoparticles as photocatalysts from biomass, offering a thorough examination. This review article provides detailed techniques for fabricating and synthesizing plasmonic nanoparticles. Furthermore, the study discusses advancements in coupling photo-oxidation alongside the hydrogen evolution mechanism for water splitting. Furthermore, prospective research topics are suggested, such as conducting a systematic analysis of photocatalysis's redox potential, developing more effective catalysts, broadening the variety of reaction types, and establishing industrial-scale photocatalytic production. Plasmonic photocatalysts have been utilized to convert biomass into H<sub>2</sub> for energy, and to explore hypothesized molecular routes for the photocatalytic oxidation of 5-hydroxymethylfurfural (HMF), which may then be converted into 2,5-furandicarboxylic acid (FDCA). This review also discusses the surface functionalization of nanophotocatalysts with –COOH, NH<sub>2</sub>, and OH groups to increase their reactivity. Reactive oxygen species (ROS) formed on the surface of nanophotocatalysts under UV or solar light play a crucial role in photocatalytic reactions. Our review has shown many challenges and difficulties related to CO<sub>2</sub> hydrogenation reactions in the presence of sustainable H<sub>2</sub>, powered by renewable energy sources. This is very critical for achieving a transition to net-zero emissions. These technologies will drive forward the development of biomass conversion processes into CO<sub>2</sub>-based fuels. This paper explores recent advancements in the conversion of biomass-derived CO<sub>2</sub> into valuable chemicals using plasmonic nanophotocatalysts. In addition to this, density functional theory (DFT) calculations also reveal how functional groups help stabilize these

Received 30th May 2024  
Accepted 14th August 2024

DOI: 10.1039/d4na00447g

rsc.li/nanoscale-advances

Indian Institute of Science Education and Research, Bhopal Bhauri, Bhopal, Madhya Pradesh-462066, India. E-mail: [agiri@iiserb.ac.in](mailto:agiri@iiserb.ac.in); Fax: +91-361-258-2292; Tel: +91-755-2692609

† Electronic supplementary information (ESI) available. See DOI: <https://doi.org/10.1039/d4na00447g>



S. Katre

*Shikha Katre is a PhD student in the Department of Chemical Engineering at IISER Bhopal. She completed her BTech in Biotechnology in 2020 and her MTech in Nanotechnology in 2022. Shikha's research interests focus on the biosynthesis of nanoparticles and their biotechnological applications across various disciplines. She enjoys spending time with family and friends, gardening, and dancing in her free time.*



P. Baghmare

*Pawan Baghmare is a PhD student in the Department of Chemical Engineering at IISER Bhopal. He completed his BTech in Biotechnology in 2020 and his MTech in Biotechnology in 2023. Pawan's research focuses on biopolymers, bioremediation, and enzymes. His doctoral research focuses on the cutting-edge fields of Biomedical Engineering and Bioremediation.*



nanoparticles and enhance electron density through photo-adsorption. This study provides a remarkable and significant review that examines current trends, future directions, and ongoing debates in this field, focusing on reaction conditions, catalyst design, and proposed mechanisms for producing valuable chemicals. These chemicals include single-carbon compounds like formaldehyde, formic acid, and methanol, as well as  $C_2^+$  compounds such as acetic acid, ethanol, methyl formate, and oxyethylene ethers. Additionally, it addresses the current state of liquid-phase  $CO_2$  hydrogenation in the presence of photocatalysts, highlighting existing challenges and potential research paths. The paper also provides an overview of the advances and challenges in the electro- and photocatalytic oxidation of HMF (hydroxymethylfurfural), detailing strategies for creating high-value chemicals through these oxidation processes. These methods, which may involve reactions like the hydrogen evolution reaction, organic substrate reduction,  $CO_2$  reduction reaction, or  $N_2$  reduction reaction, are summarized and analyzed. Furthermore, the catalytic efficiency and mechanisms of various catalyst types in these conversion systems are introduced and discussed. Electron paramagnetic resonance and scavenger studies reveal the major active species ( $\cdot OH$  and  $\cdot O_2^-$ ) in the photocatalytic conversion of biomass to different value-added products.

## Introduction

Photocatalytic nanomaterials are a specialized class of nanomaterials known for their ability to catalyse chemical reactions when exposed to light. This phenomenon, known as photocatalysis, finds extensive use in diverse fields, including environmental cleaning, energy conversion, and the development of antimicrobial coatings.<sup>1</sup> The process of photocatalysis involves the interaction between light, a photocatalyst, and reactant molecules, resulting in the acceleration of chemical transformations. When engineered at the nanoscale, these materials exhibit enhanced photocatalytic properties owing to their unique characteristics, such as high surface area and distinct electronic structures. This special characteristic makes them

particularly effective in facilitating reactions that can be challenging under normal conditions. Photocatalytic nanomaterials include various metal oxides like titanium dioxide ( $TiO_2$ ) and zinc oxide ( $ZnO$ ), as well as metallic nanoparticles such as gold (Au), silver (Ag), copper (Cu), and semiconductors like cadmium sulfide (CdS) and tungsten trioxide ( $WO_3$ ). Both metals and non-metals doped nanophotocatalysts can be used to absorb light and initiate photochemical reactions.<sup>2</sup> The photocatalytic mechanism is explained by the absorption of photons by the nanomaterial, which results in the formation of electron ( $e^-$ )-hole ( $h^+$ ) pairs. These charged carriers play a crucial role in redox reactions that involve surrounding molecules, initiating a variety of chemical modifications. This capability is utilized in applications such as degrading pollutants in water and air, generating clean energy, and producing self-cleaning or antimicrobial surfaces.<sup>3</sup> Ongoing research in the field of photocatalytic nanomaterials is dedicated to adjusting their properties, enhancing overall efficiency, and overcoming challenges to extend their practical applications in various industries. These efforts aim to realize the full potential of photocatalytic nanomaterials, contributing to sustainable solutions for environmental and energy-related challenges. Our review highlights recent advancements, such as the use of well-designed semiconductor materials and nanomaterials, which offer significant potential for selectively converting biomass under mild conditions.<sup>4</sup> For instance, semiconductor and noble metal-based nanomaterials improve biofuel efficiency and sustainability by enhancing biomass degradation and hydrogen production through the utilization of solar energy.<sup>5</sup> Additionally, advancements in nanoperculation and nanocomposite films have shown promising results in biofuel separation and stability. Moreover, innovations like the nitrogen-protected ball milling method have enhanced the photocatalytic degradation of lignocellulose, achieving remarkable conversion rates of cellulose, hemicellulose, and lignin, as demonstrated by studies.<sup>5</sup>



A. S. Giri

*Dr Ardhendu Sekhar Giri is an Assistant Professor at IISER Bhopal. He earned his PhD from IIT Guwahati in 2015, his BSc in Chemistry from the University of Calcutta, and his BTech and MTech from the same university. Dr Giri focuses on the synthesis and development of nanomaterials for use as photocatalysts in electrochemical and biological sensing and catalytic applications. The formation of chelate complexes formed*

*between pharmaceutically active compounds (PhACs) and metals, and their impact on the mineralization efficiency along with the reduction of antimicrobial activity have also been given a new flavor in this present work. Efforts are also directed towards the production of green hydrogen ( $H_2$ ) and value-added products through both photo-electrochemical water splitting and biomass conversion. As part of his doctoral work, he studied advanced oxidation processes (AOPs), which are highly efficient novel methods to accelerate the oxidation and degradation of different drug molecules from water.*



energy crops.<sup>7,8</sup> Biomass photocatalytic transformations typically occur under mild conditions. Well-designed semiconductor materials enable photon-generated carriers to selectively cleave or functionalize specific chemical bonds. This method offers greater potential for selectively converting biomass compared to traditional techniques.<sup>5</sup> Nanomaterials have become crucial in advancing biofuels and bioenergy from biomass due to their exceptional properties, such as high surface area and tailored surface chemistry. In photocatalysis, semiconductor and noble metal-based nanomaterials leverage solar energy to enhance biomass degradation, gasification, and hydrogen production, improving biofuel efficiency and sustainability. Nanopercolation employs nanomaterial-based membranes for effective separation and purification of biofuels. Nanocomposite films, combining polymers with nanofillers, enhance efficiency and stability. Nanomaterials also play a vital role in catalysis, where metallic and bimetallic catalysts improve bio-oil quality by reducing oxygen content. These advancements not only boost the effectiveness of biofuel production but also address challenges like feedstock variability and contamination.<sup>4</sup> Animal-based biomass consists of organic materials from animals, such as manure and organic waste. Additionally, microbe-based biomass involves the cultivation of microorganisms, including algae and certain bacteria, for biomass production.<sup>9</sup> The diversity of biomass sources makes it a valuable feedstock for various applications. Biomass serves multiple purposes, including energy production, the generation of fuel, and the delivery of raw materials for industrial processes. Its renewable nature shows the relatively rapid replacement of these organic materials compared to the time-scales associated with fossil fuel formation. These characteristics position biomass as a sustainable alternative that contributes to reducing dependence on finite fossil fuels and mitigating environmental impacts. In a broader context, biomass plays a crucial role in the bioeconomy, where biological resources are managed sustainably to provide food, materials, and energy.<sup>9,10</sup> This integrated approach aims to optimize the use of biological resources while maintaining ecological balance. Lignocellulosic biomass, a subset of biomass derived from plant cell walls, consists of cellulose, hemicellulose, and lignin.<sup>7</sup> Cellulose with both long chains of glucose molecules and hemicellulose is a branched polymer which is composed of several distinct sugar monomers, whereas lignin is a complex and hard polymer that provides rigidity to plant cell walls.<sup>11</sup> Among the different types of starch-based biomass, lignocellulosic biomass shows challenges in conversion due to its complex structure. However, ongoing research and technological advancements focus on overcoming these challenges, making lignocellulosic biomass a promising feedstock for the production of biofuels and other bioproducts.<sup>12</sup> Biomass, with its diverse sources and applications, contributes significantly to the transition towards sustainable and environmentally friendly energy sources. The carbon-neutral and renewable characteristics, along with the potential of lignocellulosic biomass, underscore its importance in addressing global energy and environmental challenges.<sup>13</sup>

In the realm of biomass conversion into value-added chemicals and fuels, the inclusion of nanophotocatalysts provides a possible route for boosting the overall efficacy and specificity of the conversion processes.<sup>7</sup> This cutting-edge field of research focuses on leveraging nanomaterials to catalyse chemical reactions under light irradiation, thus offering unique advantages in terms of controllability, selectivity, and efficiency. Nano-photocatalysts can be applied in the pretreatment of lignocellulosic biomass to enhance the accessibility of cellulose and hemicellulose.<sup>14</sup> This facilitates subsequent hydrolysis processes by breaking down complex polymers more efficiently.<sup>7</sup> For instance, photocatalytic pretreatment with materials such as TiO<sub>2</sub> can selectively modify the lignin structure, facilitating its removal and improving the accessibility of cellulose.<sup>15</sup> In the hydrolysis stage, nanophotocatalysts can expedite the breakdown of cellulose and hemicellulose into fermentable sugars. Semiconductor nanomaterials like TiO<sub>2</sub> can act as photocatalysts, promoting the hydrolysis process under light irradiation. Nanophotocatalysts can also improve the fermentation stage by providing a conducive environment for microorganisms. Light-assisted fermentation can improve the efficiency of sugar conversion into biofuels like ethanol or biobutanol using photocatalysts.<sup>13</sup> Nanophotocatalysts play a pivotal role in catalytic conversion processes, contributing to the transformation of sugars and intermediates into valuable chemicals and biofuels. During the upgrading of bio-oils derived from thermochemical processes, nanophotocatalysts can selectively facilitate deoxygenation and remove undesired functional groups, thus improving the quality of bio-oils.<sup>15</sup> One of the remarkable features of nanophotocatalysts is their ability to enable selective and controlled chemical transformations. By modifying the properties of nanomaterials, researchers can design catalysts that specifically target desired reactions. This selectivity is crucial for producing a range of valuable chemicals and biofuels, such as bioethanol, biobutanol, biodiesel, hydroxymethylfuran (HMF), furfural, levulinic acid, and other aromatic compounds.<sup>16</sup> The ultimate goal of integrating nanophotocatalysts into lignocellulosic biomass conversion is to produce sustainable and renewable chemicals and fuels. These bio-based products contribute to more environmentally and economically viable conversion technologies, which are crucial for the successful utilization of lignocellulosic biomass. Nanophotocatalysts, with their potential to improve reaction rate and selectivity, contribute to achieving higher overall process efficiency.<sup>15</sup> Fujishima and Honda (1972) were the first to report the water splitting by using a TiO<sub>2</sub> photoanode for hydrogen (H<sub>2</sub>) energy production.<sup>17,18</sup> Presently, it has become a revolutionary and evolving research area for clean energy production using solar or UV-light energy harvesting semiconductor materials. TiO<sub>2</sub> nanoparticles (NPs) are the most promising material as semiconductor catalysts because of their high chemical stability, non-toxicity and low-cost effectiveness. Furthermore, TiO<sub>2</sub> acts as a Lewis acid, with sites that may facilitate glucose isomerization and C<sub>3</sub> sugar dehydration, comparable to the action of Ba<sup>2+</sup>. Glucose is transformed into the fructose isomer, which is then activated and oxidized by highly oxidising active species such as <sup>•</sup>O<sub>2</sub><sup>-</sup> and <sup>•</sup>OH. The effective synthesis of



levulinic acid utilizing biomass-derived compounds (mostly C<sub>6</sub> sugars) is heavily reliant on process dynamics. C<sub>6</sub> sugar (fructose or glucose) is capable of being dehydrated and rehydrated in the presence of an acid catalyst to yield levulinic acid.<sup>19</sup> Sajid *et al.* (2021) presented the chemical pathway for upgrading C<sub>6</sub> carbohydrate to levulinic acid, as well as the activation energy required at each stage and also suggested that fructose dehydration has a larger activation energy (55.2 kJ mol<sup>-1</sup>) compared to glucose isomerization (39.8 kJ mol<sup>-1</sup>).<sup>20</sup> Li *et al.* (2023) successfully developed efficient methods for synthesizing nitrogen-containing compounds from biomass and CO<sub>2</sub>.<sup>21</sup> These compounds include urea, anilines, *N*-methylamines, imines, benzimidazoles, quinazolines, 2,3-dihydro-4(1*H*)-quinazolinones, nitriles, isoindolines, lactams, and *N*-formamides. These transformations were achieved using functional polymers (like zwitterionic polymers and COOH-functionalized ZIF-90), nanosized metal oxides, supported metal nanocatalysts, single atoms (such as Pt, Co, InO<sub>x</sub>, and Fe), and in some cases, without any catalyst (Fig. 1).

In the presence of both UV and solar light passing through the TiO<sub>2</sub> NPs, the electrons get excited from the valence band (VB) to the conduction band (CB) and the band gap energy obtained is 3.2 eV. TiO<sub>2</sub> NPs act as poor photocatalysts due to their wide band gap. Later, to enhance the photocatalytic activity of TiO<sub>2</sub> under UV-vis light, activated carbon (AC) or Zn, Cu, Ni and other metal nanoparticles like Au, Ag, Pt, Pd, *etc.*, are blended with it to reduce the band gap energy of the TiO<sub>2</sub> photocatalyst.<sup>15</sup>

Plasmonic nanostructures have demonstrated tremendous promise in photocatalysis owing to their unique photochemical

characteristics, which include strong light-matter interactions and configurable photoresponses. Considering the lower intrinsic activity of common plasmonic metals, adding highly active sites is necessary to fully realize the potential of plasmonic nanostructures in photocatalysis. A brief introduction to material fabrication and characterization techniques is followed by a detailed discussion of the synergy between plasmonic nanostructures and active sites in photocatalysis. In the form of local electromagnetic fields, hot carriers, and photothermal heating, active sites can facilitate the connection of solar energy captured by plasmonic metals to catalytic processes.

Jose *et al.* (2013) synthesized the Au/TiO<sub>2</sub> nanocomposite by using the solvated metal atom dispersion (SMAD) method.<sup>22</sup> These nanocomposite photocatalysts were then utilized for hydrogen production from ethanol or methanol under UV-visible radiation. When UV or solar radiation illuminates the TiO<sub>2</sub> NPs, electrons get transferred from the conduction band (CB) of TiO<sub>2</sub> to Au nanoparticles (AuNPs) and then these electrons get photoexcited from AuNPs, leading to a decrease in the energy band gap from 3.2 eV to 2.5 eV. Thus, by doping metallic nanoparticles with TiO<sub>2</sub> NPs, they show better photocatalytic activity.

Wang *et al.* (2015) showed that incorporating AuNPs into TiO<sub>2</sub> nanofibers supported by H-form Y-zeolites led to increased cellulose hydrolysis efficiency under visible light.<sup>14</sup> This plasmonic nanostructure efficiently absorbed visible light through the supported AuNPs on active zeolite catalysts, facilitating direct light-catalyst interaction and minimizing heating of the solvent system. Their research investigated into how reaction parameters like temperature, light intensity, and wavelength influenced cellulose conversion to valuable chemicals.

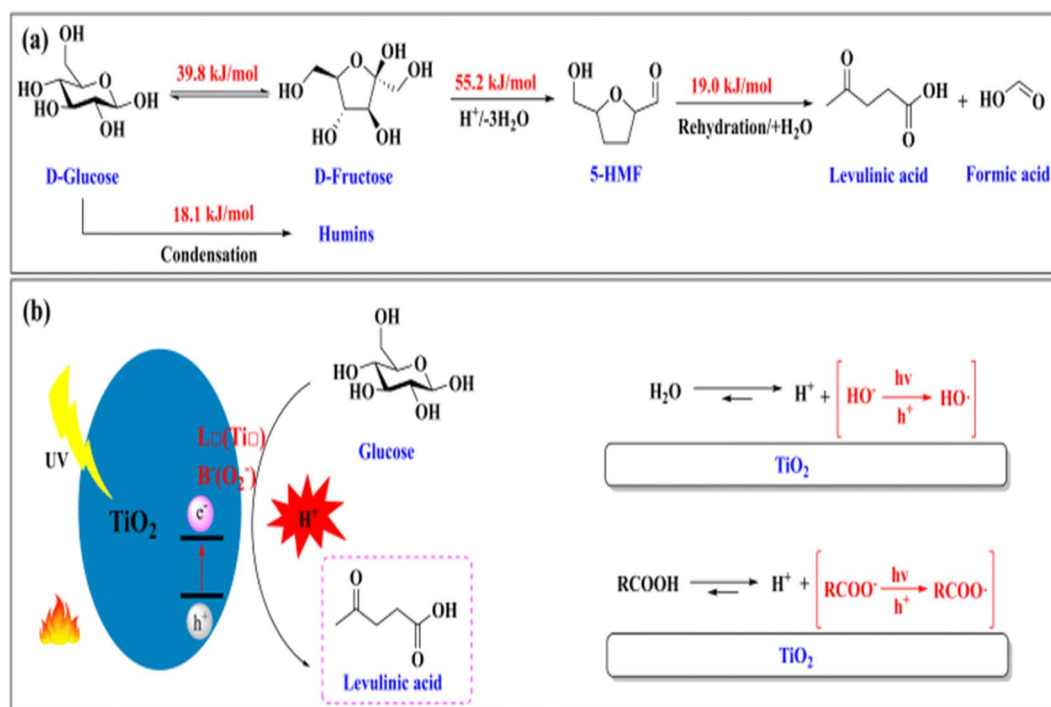


Fig. 1 (a) The reaction pathway illustrating the conversion of glucose to levulinic acid, including the activation energy at each stage. (b) Mechanism of conversion of glucose into levulinic acid mediated by TiO<sub>2</sub> photocatalysis.<sup>19</sup>



Markedly, glucose and HMF yields exceeded 60% at 130 °C after 24 hours under mild conditions. The study emphasized the critical roles of acid strength and the localized surface plasmon resonance (LSPR) effect of AuNPs in processing efficiency. Furthermore, they proposed a mechanism highlighting how the LSPR effect enhanced acid strength *via* the polarized electrical fields of zeolites. These findings offer promising avenues for reducing processing costs, energy consumption, and advancing the renewable utilization of biomass resources in biofuel and chemical production.<sup>14</sup>

In the presence of powdered TiO<sub>2</sub> photocatalysts synthesized by the ultrasound promoted sol-gel method, glucoses underwent oxidation. Compared to the widely known Degussa P-25 photocatalyst, these catalysts were more selective for glucaric acid, gluconic acid and arabitol, with approximately 70% selectivity. Operating under mild conditions of 30 °C, atmospheric pressure, and very short reaction times (within 2 min to 5 min), the photocatalytic systems demonstrated significant selectivity towards valuable molecules. The physiological properties of novel TiO<sub>2</sub> materials, *e.g.*, a large particular surface area, nanoscale anatase phase and clear light absorption, along with optimised reaction conditions contribute to this increased selectivity.<sup>9,13</sup> These value-based chemicals are utilised in various areas like food, pharmaceuticals, *etc.*

Zhou *et al.* (2017) investigated the importance of converting biomass derived compounds into value added chemicals.<sup>15</sup> The study examines the selective photooxidation of various biomass derived chemicals, such as ethanol, xylose, 5-hydroxycarboxylic acid, glucose, 2-furaldehyde and furfural alcohol, into their corresponding carboxylic acid compounds by means of atmospheric air at room temperature. It has been observed that AuNPs blended with TiO<sub>2</sub> (AuNPs/TiO<sub>2</sub>) proficiently facilitated these reactions under both UV and visible light in a Na<sub>2</sub>CO<sub>3</sub> aqueous solution, yielding appropriate chemicals like acetic acid, gluconic acid, xylose acid, 2-furoic acid, 2,5-furan dicarboxylic acid and 2-furoic acid from their respective biomass derived compounds.<sup>23</sup> Under optimized conditions, the selectivities for desired products exceeded 95% in all reactions. Detailed investigations revealed that the visible-light-responsive activity was attributed to the surface plasmonic resonance of AuNPs, while the UV-light-responsive activity stemmed from the band-gap photoexcitation of TiO<sub>2</sub>. Na<sub>2</sub>CO<sub>3</sub> played a dual role as a promoter for visible-light-induced oxidation and as an inhibitor of reactive oxygen species with potent oxidation capabilities under UV light, as shown in Table 1.<sup>23,24,31</sup>

Giannakoudakis *et al.* (2019) demonstrated that HMF stands out as a significant chemical resource, easily sourced from lignocellulosic biomass, and shows potential as a precursor for polymer or fuel creation.<sup>16</sup> By focusing on the partial oxidation of HMF's hydroxyl group, we can produce 2,5-diformylfuran (DFF), which holds significant promise across various biochemical industries. They introduced newly developed manganese(IV) oxide nanorods as catalysts for this partial oxidation process, effectively functioning under standard conditions. The nanocatalyst operates effectively with low light energy and without additional chemicals, displaying exceptional selectivity as a photo-assisted catalyst. Under optimal

conditions, it achieved over 99% conversion of HMF with nearly 100% selectivity towards DFF.<sup>15</sup> Molecular oxygen plays a pivotal role in facilitating selective oxidation, while utilizing an aprotic and less polar organic solvent, such as acetonitrile, instead of water, further bolsters catalyst reactivity.<sup>24</sup>

The process showed utilizing ultra-thin CdS nanosheets decorated with nickel (Ni/CdS) to drive the photocatalytic conversion of key intermediate chemicals derived from biomass, such as furfural alcohol and HMF, into valuable compounds like aldehydes and acids. Furthermore, these biomass-derived intermediates acted as proton sources, facilitating simultaneous H<sub>2</sub> production upon visible light exposure under ambient conditions.<sup>25</sup> A notable disparity in the transformation rates of furfural alcohol and HMF into their respective aldehydes in neutral water was observed and scrutinized. Theoretical calculations indicated that the slightly stronger binding of the aldehyde group in HMF to Ni/CdS led to a lower conversion of HMF to 2,5-diformylfuran compared to the conversion of furfural alcohol to furfural. Nonetheless, under alkaline conditions, the photocatalytic oxidation of furfural alcohol and HMF resulted in complete conversion to the corresponding carboxylates alongside concurrent H<sub>2</sub> production.<sup>37</sup>

This review begins by outlining the advancements made in research regarding various porous carbon materials such as activated carbon (AC), doped carbon, carbon molecular sieves (CMS), and others, specifically focusing on their application in flue gas carbon capture. Additionally, it discusses progress made in utilizing porous carbon for direct carbon capture from air, particularly targeting lower CO<sub>2</sub> concentrations.<sup>26</sup> Furthermore, it delves into critical considerations when employing porous carbon for practical carbon capture applications, including the impacts of humidity, temperature, and flow rate. The aim is to offer valuable insights for the development of porous carbon-based adsorbents with real-world applicability.

This review provides an overview of recent advancements in research concerning porous carbons for carbon capture from both flue gas and directly from air over the past five years. It encompasses various porous carbon materials such as activated carbon (AC), heteroatom-modified porous carbon, carbon molecular sieves (CMS), and others. The focus is on understanding how parameters like temperature, water content, and gas flow rate in industrial flue gas affect the performance of porous carbon adsorbents.<sup>27</sup> Furthermore, it summarizes the different preparation methods for porous carbons and explores environmentally friendly approaches while enhancing CO<sub>2</sub> adsorption capacity and selectivity. By analyzing the impact of real industrial flue gas on adsorbents, the review offers novel insights and evaluation methods for the development and preparation of porous carbon materials.

This review systematically outlines recent progress in the photocatalytic conversion of biomass-derived organic heterocyclic compounds into valuable products. Extensive research has been conducted on the oxidation of these compounds, particularly the conversion of HMF to DFF, utilizing various materials such as TiO<sub>2</sub> and perovskite-type materials. However, challenges persist, including unsatisfactory selectivity of DFF due to the generation of highly reactive species leading to



Table 1 Biomass conversion to fuels and chemicals<sup>23,24</sup>

Biomass derived compounds	Nano-photocatalyst	Light	Product	References
Cellulose	Au-HYT	Visible light	Glucose	14
Cellulose	Ir/HY <sub>3</sub>	Xenon lamp	Cellobiose	25
Cellulose	P25-SO <sub>4</sub> <sup>2-</sup> -Ni <sub>x</sub> S <sub>y</sub>	Xenon lamp	H <sub>2</sub>	26
Cellulose	TiO <sub>2</sub> /NiO <sub>x</sub> @Cg water	Xenon lamp	H <sub>2</sub>	27
Rice straw	ZnO NPs	—	Ethanol	28
Paulownia elongata	Zn-doped SnO <sub>2</sub> NPs	Xenon lamp	Hydrogen	29
Sugarcane bagasses	Fe <sub>3</sub> O <sub>4</sub> NPs	Light intensity	Hydrogen	24
Rice straw	Sulphonated graphene	—	Biogas methane	30
Miscanthus biomass	Zeolites coated TiO <sub>2</sub> NPs	UV	Methane	31
Corn cob	CeFe <sub>3</sub> O <sub>4</sub> NPs	—	Methane	32
Potato peels	NiO NPs and Fe <sub>3</sub> O <sub>4</sub> NPs	—	Bioethanol	33
Lignocellulose	TiO <sub>2</sub> (ST-01)	UV	Ethanol and CO <sub>2</sub>	34
Lignin	TiO <sub>2</sub>	UV	Syringaldehyde	35
Lignin	Pt/Bi-TiO <sub>2</sub> (P25)	Solar light	Vanillic acid	36

overoxidation of intermediates.<sup>28</sup> Additionally, achieving low HMF conversion is crucial for optimizing the reaction. The review also discusses studies focusing on substituting the oxygen evolution reaction (OER) in photocatalytic water splitting with biomass-based photooxidation, which enhances the economic value and efficiency of the overall process. Furthermore, it summarizes a few studies exploring the photooxidation of HMF to alternative products and the photoreduction of furanic compounds.

## Sources of biomass

Biomass denotes natural substances obtained from plants and animals, suitable for generating energy. There are several sources of biomass, each with its own characteristics and potential uses. Here are some common sources of biomass:

(1) Wood and agricultural residues: wood is one of the oldest and most widely used biomass resources. It can come from forests, logging residues, sawdust, and wood processing industries. Agricultural residues such as corn stover, rice husks, wheat straw, and sugarcane bagass are also abundant sources of biomass.<sup>38</sup>

(2) Energy crops: certain crops are specifically grown for biomass energy production. These include fast-growing plants like switchgrass, miscanthus, willow, and poplar trees. These energy crops can be cultivated on marginal lands not suitable for food crops and harvested for biomass.<sup>39</sup>

(3) Organic waste and animal waste: various forms of organic waste generated from households, industries, and agriculture can be used as biomass feedstock. This includes food waste, animal manure, sewage sludge, and municipal solid waste. Animal waste, such as manure, and by-products from meat and dairy industries can be used as biomass feedstock. Anaerobic digestion of animal waste can produce biogas for heat and power generation. Anaerobic digestion and composting are common methods to convert organic waste into biogas and compost, respectively (Dominik *et al.*, 2013).<sup>40</sup>

(4) Algae: algae are photosynthetic microorganisms that can grow rapidly in water and sunlight. They can be cultivated in ponds, bioreactors, or open water systems for biomass

production. Algae can yield oils suitable for biodiesel production, as well as proteins and carbohydrates and cosmetics and for various other applications (Chojnacka *et al.*, 2018).<sup>41</sup>

(5) Aquatic biomass: aquatic plants and organisms such as seaweeds, water hyacinths, and aquatic weeds can be harvested from oceans, lakes, and rivers for biomass production. These resources can be utilized for biofuel production, bioremediation, and other purposes (Namasivayam *et al.*, 2023 & Bharathiraja *et al.*, 2015).<sup>42,43</sup>

(6) Urban biomass: urban areas generate significant amounts of biomass in the form of yard waste, landscape trimmings, and municipal solid waste. These organic materials can be collected and processed to produce biogas, compost, or converted into biofuels through various technologies (Li *et al.*, 2017).<sup>44</sup>

(7) Forest residues: besides wood, forests produce other biomass residues such as branches, bark, and leaves. These residues can be collected sustainably without affecting forest ecosystems and utilized for energy generation or other applications.<sup>45</sup>

Each biomass source has its own advantages and challenges in terms of availability, sustainability, and conversion technologies. The choice of biomass source depends on factors such as local resources, environmental considerations, and the intended end use of the biomass (Fig. 2a and b).

### Wood as a source of biomass

Wood is one of the most traditional and widely used sources of biomass. Biomass refers to organic materials, such as plants and trees, which can be used to produce energy through various processes. Wood biomass is derived from trees and woody plants, and it can be utilized in several forms for energy generation.<sup>46</sup> Wood biomass is considered a renewable energy source because trees can be replanted and grown to replace those harvested for biomass production. However, it's crucial to manage wood biomass resources sustainably to avoid deforestation and ensure the long-term environmental benefits of using biomass for energy. Wood is a complex natural material composed primarily of three main constituents: cellulose, hemicellulose, and lignin,<sup>47</sup> along with smaller amounts of



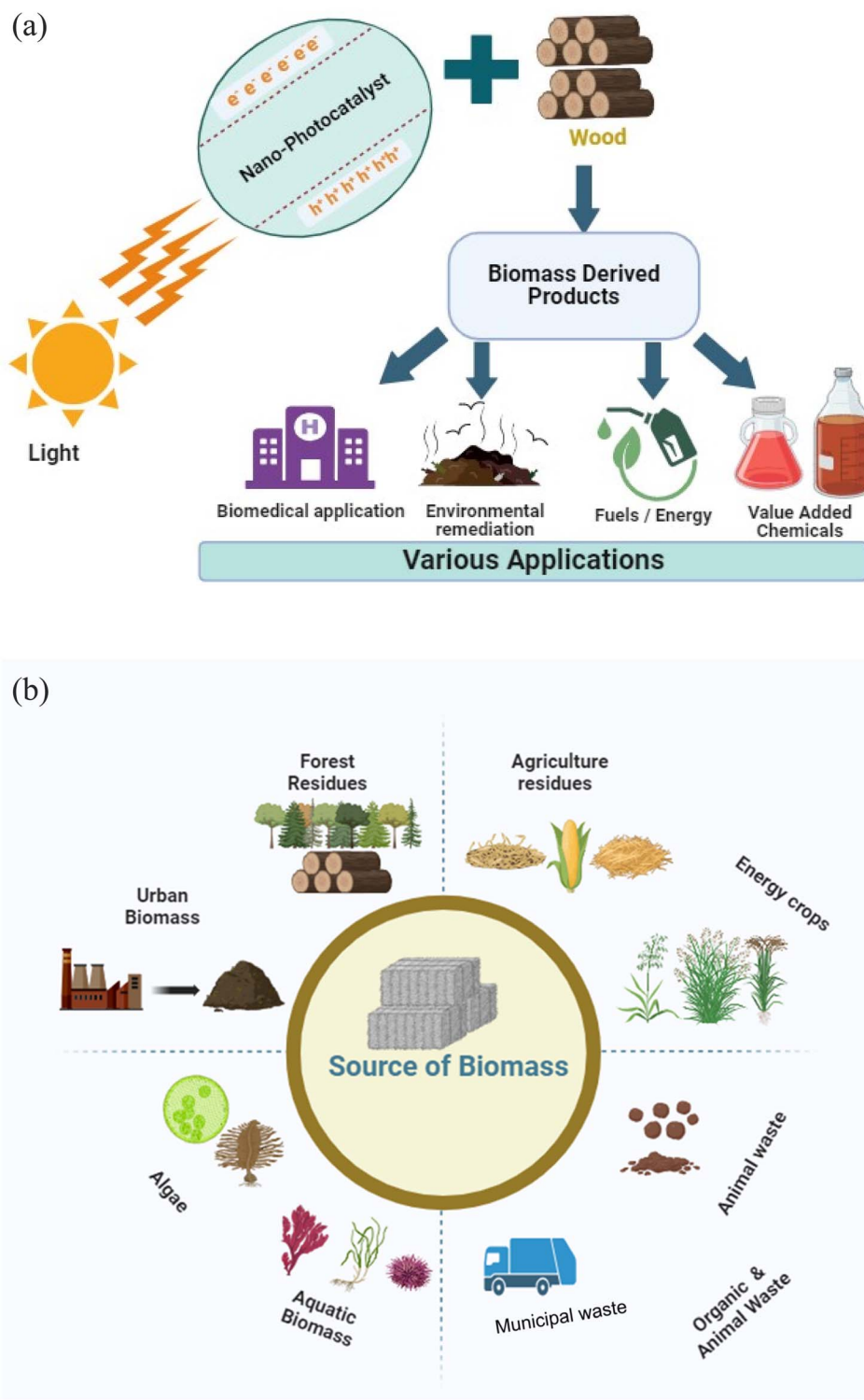


Fig. 2 (a) Conversion and application of wood biomass through a nanophotocatalyst. (b) Different sources of biomass.

extractives, such as resins, tannins, and waxes. Each constituent plays a crucial role in the structure, function, and properties of wood. Cellulose is the most abundant organic polymer on Earth and the primary structural component of wood. It forms long chains of glucose molecules linked together, providing strength and rigidity to the cell walls of wood fibers.<sup>48</sup> Cellulose molecules are arranged in a crystalline structure, contributing to the

overall stiffness and mechanical properties of wood. Cellulose also plays a vital role in water transport within the wood structure.<sup>48</sup> Hemicellulose is a complex branched polymer composed of various sugar units, including xylose, glucose, mannose, and galactose.<sup>49</sup> Unlike cellulose, hemicellulose is amorphous, meaning it lacks a defined crystalline structure. Hemicellulose acts as a cementing material between cellulose



fibers, binding them together and providing cohesion to the wood structure.<sup>50,51</sup> It also serves as a source of energy for microorganisms during wood decay and contributes to the hydrophilic properties of wood.<sup>52</sup> Lignin is a complex phenolic polymer that fills the spaces between cellulose and hemicellulose in the cell walls of wood fibers. It provides structural support and rigidity to wood, particularly in hardwood species.<sup>48,53</sup> Lignin is highly resistant to microbial degradation and plays a crucial role in the natural defense mechanisms of trees against pathogens and pests. However, lignin also poses challenges in wood processing and pulping due to its recalcitrance and tendency to interfere with fiber bonding.<sup>54</sup> Extractives are organic compounds found in wood that are not part of the main structural components (cellulose, hemicellulose, and lignin). Wood extractives are natural compounds that occur outside the cell wall of lignocellulose. Although they are located within the cell wall, they do not form chemical bonds with it. These substances can be classified into three primary groups according to their chemical composition: aromatic phenolic compounds, aliphatic compounds such as fats and waxes, and terpenes and terpenoids.<sup>55</sup> They include a wide range of substances such as resins, gums, tannins, oils, and waxes.<sup>56</sup> Extractives contribute to the colour, odour, and chemical properties of wood and play roles in natural defence against decay, insect attacks, and environmental stresses.<sup>57</sup> Extractives can also affect the processing and properties of wood products, influencing characteristics such as durability, weather resistance, and adhesive bonding.<sup>58,59</sup> Understanding the composition and properties of these wood constituents is essential for various applications, including wood processing, pulping,

papermaking, bioenergy production, development of wood-based materials and value-added products.<sup>60</sup> Additionally, the proportions and distribution of these constituents vary among different wood species and can influence the overall properties and performance of wood materials.

### Rice husk as a source of biomass

Rice husk is the outer covering of the rice grain, also known as rice hull. The rice husk is separated from the rice grain during milling, leaving behind the edible rice kernel. Rice husk is abundantly available as a by-product of rice milling.<sup>61</sup> Rice husk is primarily composed of cellulose, hemicellulose, lignin, and silica, along with smaller amounts of other organic and inorganic compounds.<sup>62</sup> Rice husk is a valuable biomass fuel and it can be burned to generate electricity or heat in biomass power plants.<sup>63</sup> The combustion of rice husk is considered environmentally friendly because it is a renewable resource and emits fewer greenhouse gases compared to fossil fuels. Rice husk can be converted into biochar through pyrolysis or gasification processes. Biochar is a type of charcoal used for soil improvement, carbon sequestration, and as a component of composite materials.<sup>64</sup> Processed rice husk can be used as an eco-friendly insulation material in construction. It offers good thermal insulation properties and can be used in panels or bricks.<sup>65</sup> Rice husk contains a high concentration of silica, which can be extracted and used in various industrial applications such as in the production of silicon compounds, ceramics, and high-performance concrete.<sup>66</sup> Rice husk biomass can be used as a soil additive to improve water retention, soil structure and aeration. It helps in controlling soil pH and can be particularly

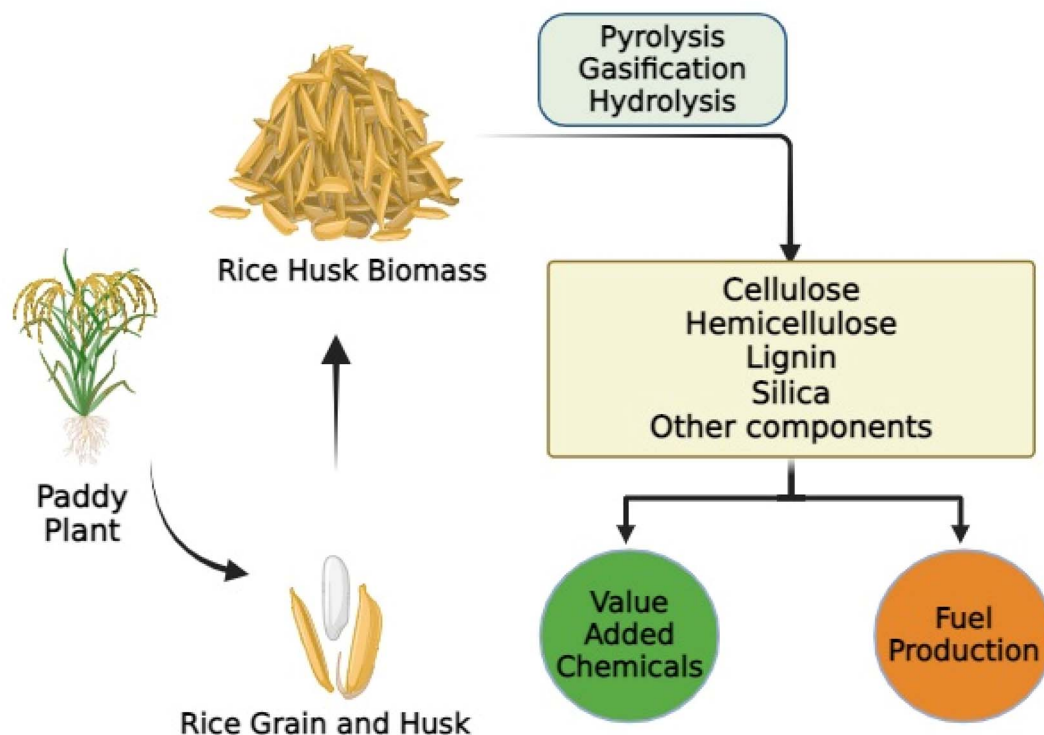


Fig. 3 Rice husk as a biomass source.



beneficial in areas with poor soil quality.<sup>67</sup> Rice husk is a versatile biomass resource with various applications across different industries, contributing to sustainable development and waste reduction in rice-producing regions (Fig. 3).

## Preparation of biomass

### Preparation of biomass from wood

Preparing biomass from wood involves several steps depending on the intended use and the desired form of biomass. Here is a general methodology for preparing biomass from wood:

**Feedstock selection:** choose appropriate wood feedstock based on factors such as species, moisture content, size, and availability. Common feedstocks include forestry residues, sawmill waste, logging slash, and dedicated energy crops like willow or poplar.<sup>68–70</sup>

**Collection and transportation:** harvest or collect the wood feedstock from forests, logging sites, or other sources. Transportation may involve chipping or grinding larger pieces of wood to facilitate handling and reduce transportation costs.<sup>71,72</sup>

**Size reduction:** depending on the application, the wood feedstock may need to be further processed to reduce its size. This can involve chipping, grinding, or shredding the wood into smaller pieces or particles. Smaller particle sizes increase the surface area and improve the efficiency of subsequent processing steps.<sup>73</sup>

**Drying:** wood feedstock typically contains a significant amount of moisture, which can reduce the energy content and efficiency of biomass conversion processes. Drying the wood to

reduce moisture content is often necessary. This can be done using various methods such as air drying, kiln drying, or mechanical drying.<sup>74</sup>

**Palettization or briquetting:** if the biomass is intended for use in pellet stoves, boilers, or briquette presses, it may need to be further processed into densified forms such as wood pellets or briquettes. This involves compressing the dried wood particles under high pressure to form dense, uniform products with standardized shapes and sizes.<sup>75</sup>

**Chemical treatment:** in some cases, wood biomass may be subjected to chemical treatment to enhance its properties or improve its suitability for specific applications. For example, torrefaction or hydrothermal carbonization can be used to increase the energy density and stability of biomass.<sup>76,77</sup>

By following these steps and considering specific requirements and constraints, wood biomass can be effectively prepared for various applications, including energy generation, biofuel production, and agricultural uses (Fig. 4).

### Preparation of biomass from rice husk

The preparation of biomass from rice husk typically involves several steps to convert the raw husk into a usable form for various applications. Here's a general outline of the process:

**Collection and storage:** rice husk is collected from rice mills where it is produced as a byproduct of the rice milling process. It's important to properly store the husk to prevent contamination and maintain its quality.<sup>78</sup>

**Cleaning and drying:** the collected rice husk may contain impurities such as dust, dirt, and small debris. It is usually

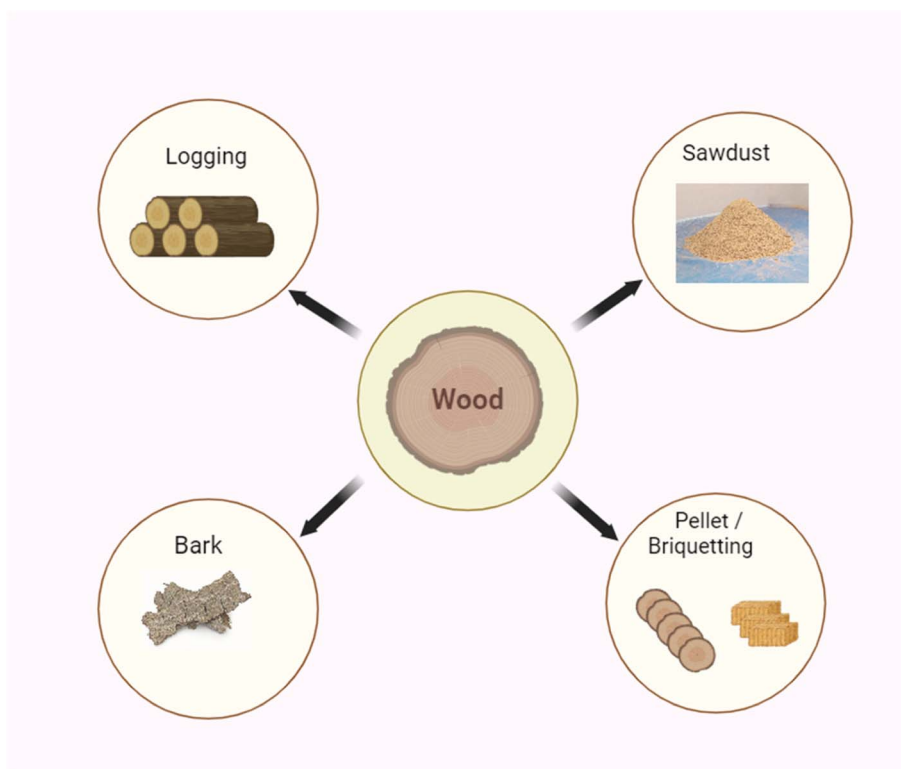


Fig. 4 Wood as a biomass source and its form.



cleaned to remove these impurities. After cleaning, the husk is dried to reduce its moisture content. Drying can be done using natural sunlight or mechanical drying methods.<sup>79</sup>

**Size reduction:** rice husk is often too large in size for certain applications, so it's shredded or ground into smaller particles. This process facilitates handling and improves the efficiency of subsequent processing steps.

**Pyrolysis or gasification:** one common method for converting rice husk into biomass is through pyrolysis or gasification. In pyrolysis, the husk is heated in the absence of oxygen to break it down into biochar, bio-oil, chemicals and syngas.<sup>80</sup> Gasification involves partially oxidizing the husk at high temperatures to produce syngas, which can be used as a fuel.<sup>81</sup> These processes require specialized equipment and controlled conditions.

## Fundamental principles behind various plasmonic nanomaterials

Photocatalytic nanomaterials have garnered significant attention due to their ability to harness solar energy and drive chemical reactions, particularly in environmental remediation and energy conversion applications.<sup>82</sup> The fundamental principles of these materials lie in their unique structural and chemical properties that enable them to absorb light and promote catalytic reactions. Here are some key fundamental principles of various photocatalytic nanomaterials:

**Bandgap energy:** photocatalytic nanomaterials typically have semiconductor properties, meaning they have a bandgap that determines their ability to absorb light. The bandgap energy determines which wavelengths of light the material can absorb,

and thus its photocatalytic activity. Materials with bandgaps matching the solar spectrum (visible light) are desirable for efficient photocatalysis as shown in Fig. 5.<sup>83,84</sup>

**Charge carrier generation and separation:** when a photocatalytic nanomaterial absorbs light, it generates electron-hole pairs (excitons).<sup>85</sup> Efficient charge carrier generation and separation are crucial for preventing their recombination, which can reduce photocatalytic efficiency.<sup>86</sup> Nanomaterials with suitable energy levels and structural features facilitate rapid charge separation, typically through the creation of heterojunctions or by incorporating co-catalysts.<sup>87</sup>

**Surface reactivity:** the surface of photocatalytic nanomaterials plays a vital role in catalyzing chemical reactions. Active sites on the surface where reactants can adsorb and undergo reactions are essential for efficient photocatalysis. Nanomaterials with high surface area-to-volume ratios, such as nanoparticles and nanowires, provide more active sites (Fig. 6), leading to enhanced catalytic activity.<sup>29,88</sup>

**Redox properties:** photocatalytic reactions involve redox processes, where electron transfer occurs between the photocatalyst and reactants. The redox properties of the nanomaterial, including the energy levels of its valence and conduction bands, determine its ability to facilitate these electron transfer reactions.<sup>89</sup> Tailoring the composition and surface chemistry of nanomaterials can modify their redox properties to enhance photocatalytic performance.<sup>90,91</sup>

**Stability and durability:** photocatalytic nanomaterials must maintain their structural and chemical integrity under prolonged exposure to light and reactive species. Materials with high stability and durability exhibit long-term photocatalytic

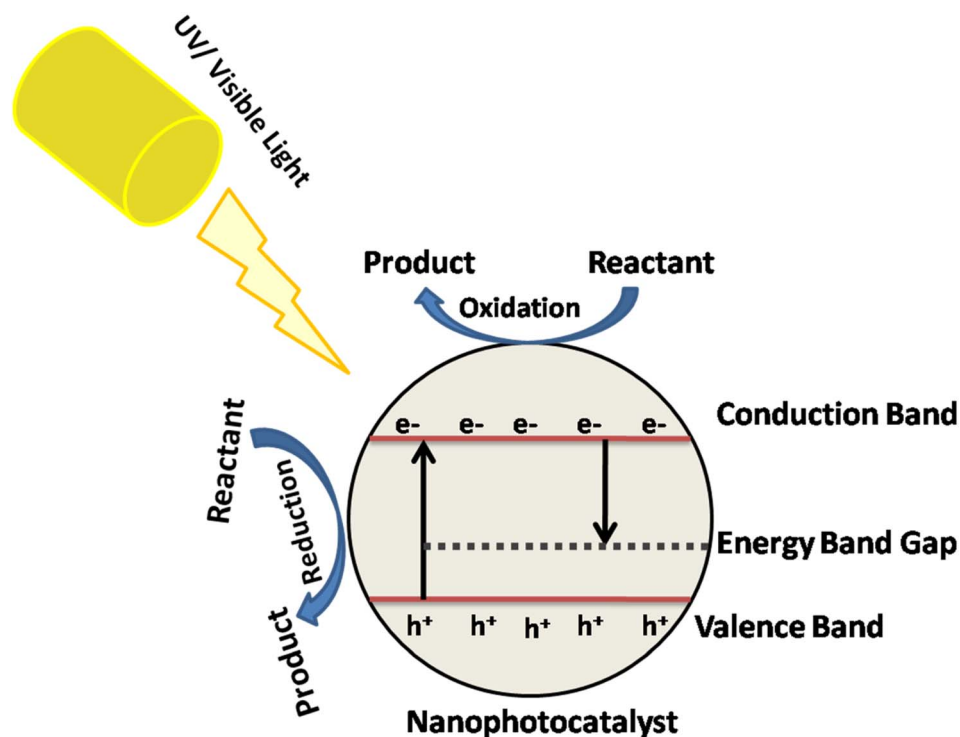


Fig. 5 Nanophotocatalyst band gap energy.



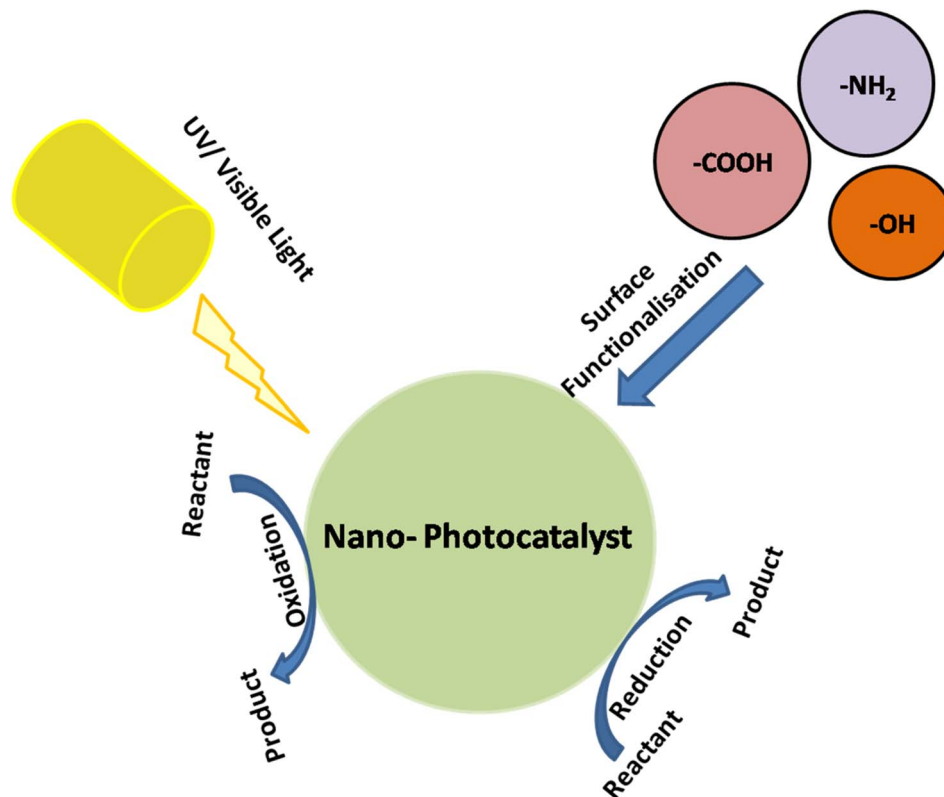


Fig. 6 Surface functionalization of nano-photocatalysts with  $\text{-COOH}$ ,  $\text{NH}_2$ , and  $\text{OH}$  groups to enhance their reactivity.

activity without undergoing degradation or structural changes. Engineering nanomaterials with suitable surface coatings or doping strategies can improve their stability and durability.<sup>29,92</sup>

Reactivity towards target molecules: the specific photocatalytic activity of nanomaterials depends on their reactivity towards target molecules involved in the desired chemical transformations. Tailoring the composition, morphology, and surface functionalization of nanomaterials can enhance their selectivity towards specific reactants or pollutants, enabling targeted photocatalytic applications.<sup>93,94</sup> By understanding and optimizing these fundamental principles, researchers can design and develop photocatalytic nanomaterials with improved performance for various applications, including pollutant degradation, water splitting for hydrogen production, and carbon dioxide reduction.<sup>94,95</sup> Continued advancements in nanomaterial synthesis and characterization techniques are driving the exploration of new materials and the refinement of existing ones for more efficient photocatalysis (Fig. 7).

## Synthesis of plasmonic nanomaterials

### Au/TiO<sub>2</sub> plasmonic NPs

Gold (Au) nanoparticles blended with titanium dioxide (TiO<sub>2</sub>) represent a nanophotocatalyst system with remarkable properties. Au/TiO<sub>2</sub> nanophotocatalysts leverage the unique characteristics of both materials, offering enhanced photocatalytic activity for various applications. Due to the wide band gap energy of TiO<sub>2</sub>, it was considered a poor photocatalyst. However,

by blending TiO<sub>2</sub> with Au nanoparticles, the band gap energy can be decreased. Kholikov *et al.*, 2021, reported that the hydrothermal synthesis method successfully produced high photocatalytic activity anatase TiO<sub>2</sub>, with modified Au nanoparticles facilitating enhanced degradation of 2,4-dichlorophenol.<sup>96</sup> Their research confirms the excellent visible light photo-activity of the Au/TiO<sub>2</sub> nanocomposite, which is attributed to Au's surface plasmon resonance (SPR) modification and catalytic function, which extends visible light response and facilitates electron transfer from SPR Au to TiO<sub>2</sub>.<sup>97</sup> Adjusting the photogenerated electrons on TiO<sub>2</sub>-based nano-photocatalysts effectively enhances charge separation, providing a comprehensive strategy for highly efficient photocatalytic degradation of pollutants. Veziroglu *et al.*, 2020, demonstrated that a highly active TiO<sub>2</sub> substrate enables precise deposition of Au nanoclusters (NCs), with solvent type and illumination time being crucial for achieving optimal surface coverage on TiO<sub>2</sub>, impacting photocatalytic efficacy.<sup>98</sup> Balancing electron storage capacity and optical absorption *via* controlled surface coverage of Au NCs on TiO<sub>2</sub> is essential for enhanced performance. For instance, low surface coverage of Au NCs significantly boosts TiO<sub>2</sub> optical absorption at UV wavelengths, improving photocatalytic activity. This straightforward method offers a pathway for the simple fabrication of Au-TiO<sub>2</sub>-based catalytic and sensor devices (Fig. 8).

**Deposition-precipitation method.** TiO<sub>2</sub> nanoparticles were synthesized *via* the sol-gel method by mixing  $\text{Ti}(\text{OBU})_4$  and ethanol, and then this mixture was added dropwise into



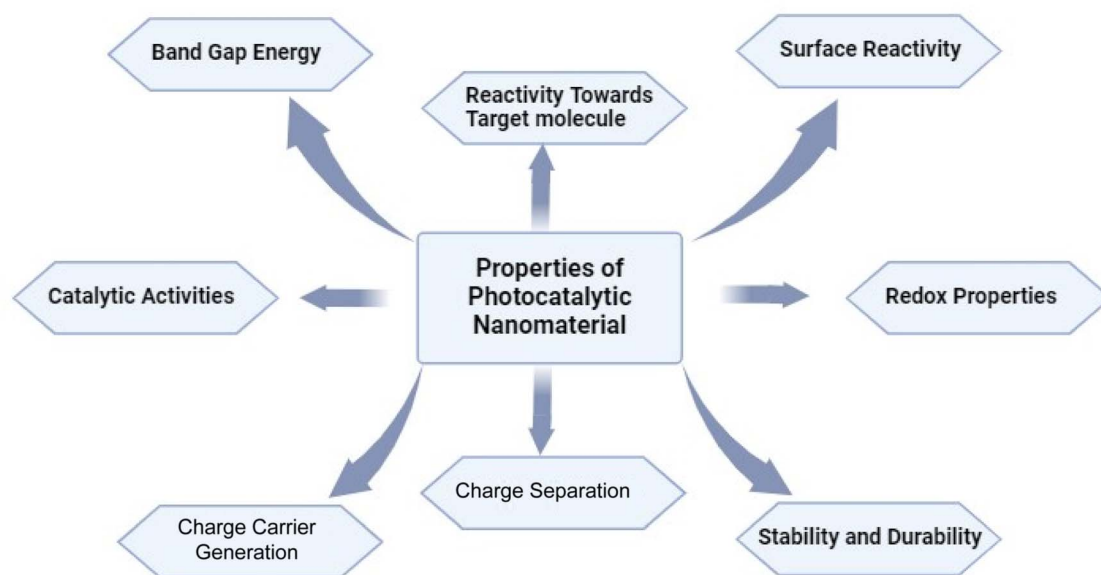


Fig. 7 Properties of photocatalytic nanomaterials.

a solution containing ethanol, deionized water (D. I.), and  $\text{HNO}_3$ . After heating and cooling, the resulting precipitates were washed with D. I. water and ethanol, and then dried and calcined.<sup>96</sup> Gold (Au) deposition on the  $\text{TiO}_2$  nanoparticles was achieved using a deposition-precipitation method with  $\text{HAuCl}_4 \cdot 4\text{H}_2\text{O}$ . The pH of the solution was neutralized with  $\text{NaOH}$ , followed by washing and calcination of the products (Fig. 9).

**Sonochemical reduction method.** According to Gupta *et al.*, 2016, the sonochemical reduction method, conducted in an ultrasonication bath, offers the advantage of avoiding post-synthesis treatments such as washing and drying.<sup>99</sup> Mizukoshi *et al.* (2006) demonstrated that this method facilitates the deposition of metal nanoparticles onto support materials.<sup>100</sup> During sonolysis, organic species break down into smaller

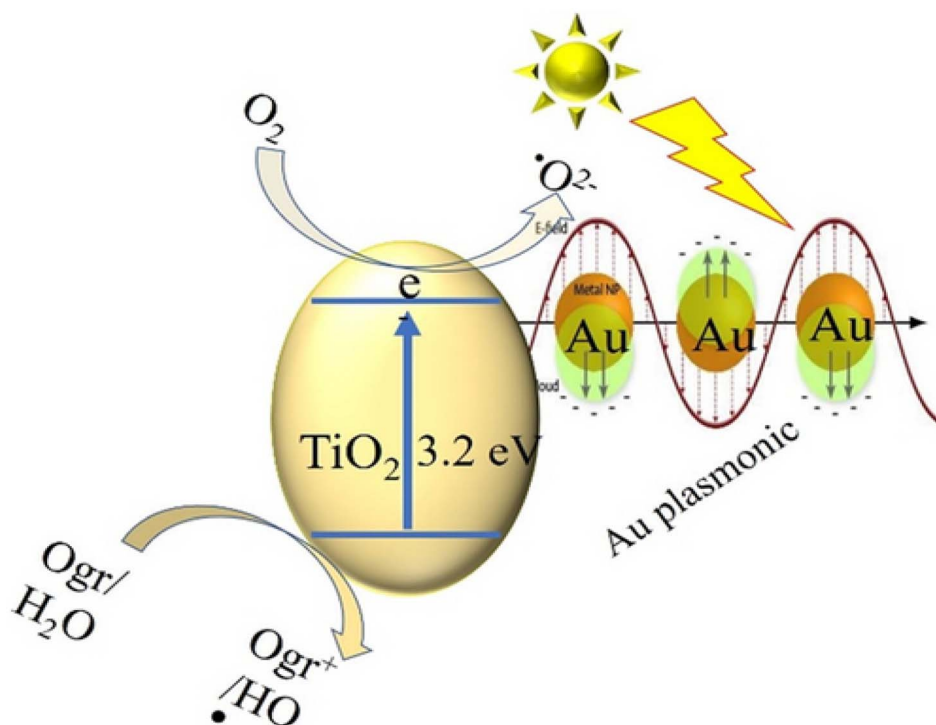


Fig. 8 Au doped  $\text{TiO}_2$  nano-photocatalyst. Adapted from Copyright JCCS, Wiley 2021.<sup>96</sup>



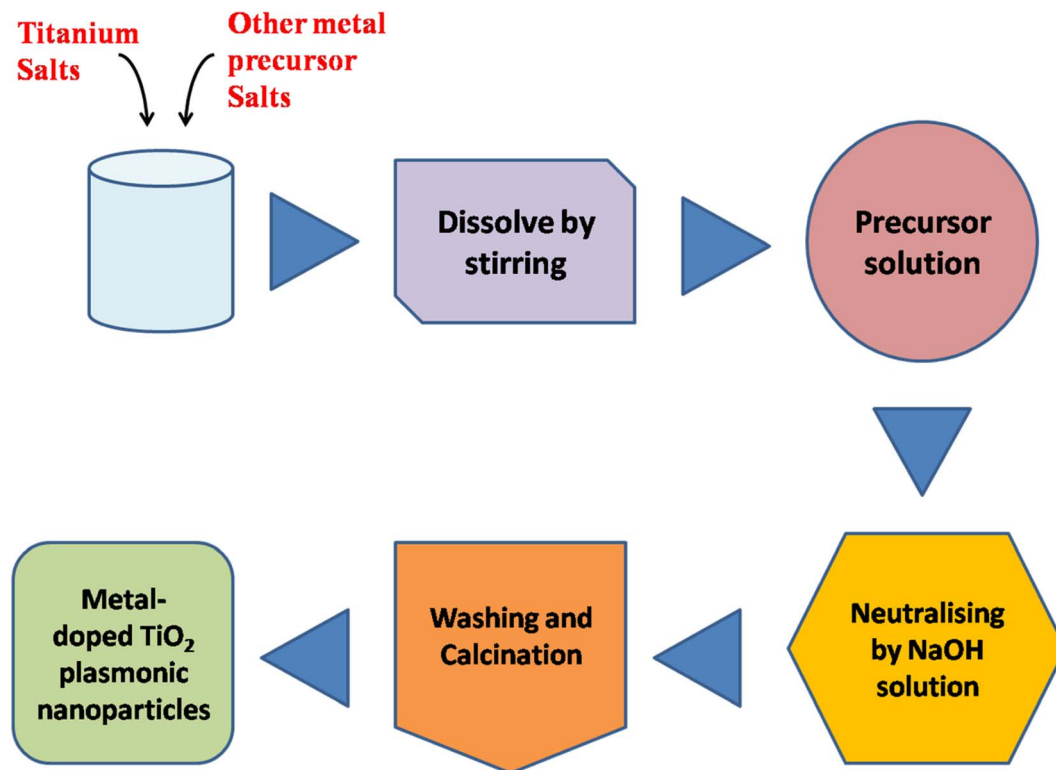


Fig. 9 Deposition-precipitation method for the synthesis of metal-doped TiO<sub>2</sub> nanomaterials.

fragments, acting as initiators for the reduction of metal salts. Mizukoshi *et al.* (2006) successfully immobilized various metal nanoparticles on TiO<sub>2</sub> surfaces using the sonochemical method (Fig. 10) in the presence of polyethylene glycol monostearate and with a brief application of input power.<sup>100</sup>

**Impregnation method.** The Au-TiO<sub>2</sub> nanoparticles were synthesized using the conventional incipient impregnation method. TiO<sub>2</sub> was placed in a round-bottom flask and exposed to a solution of dissolved HAuCl<sub>4</sub>, with vigorous agitation for 30 minutes, followed by solvent stirring using a rotary evaporator.<sup>101</sup> After drying, the sample was subjected to heating at an ideal temperature for several hours, followed by a reduction heat treatment in a hydrogen environment. The temperature was gradually increased at a rate of 2 °C per minute until it reached 350 °C, where it was held for several minutes. Variations in pH (alkaline, neutral, and acidic) were tested, and the prepared samples were characterized to assess their different properties<sup>102</sup> (ESI Fig. S1†).

**Sol-gel method.** The sol-gel approach entails the hydrolysis and condensation of metal alkoxides, such as titanium isopropoxide, to form a sol that contains TiO<sub>2</sub> precursors (titanium chloride or titanium isopropoxide). Gold precursors (auric chloride) can be introduced into the sol either by direct addition or by impregnating the TiO<sub>2</sub> sol with a solution of the gold precursor. The resulting mixture is then subjected to gelation and further processing, such as drying and calcination, to obtain the Au/TiO<sub>2</sub> composite material<sup>103</sup> (ESI Fig. S2†).

**Hydrothermal/solvothermal method.** This method involves the synthesis of Au/TiO<sub>2</sub> nanocomposites under high pressure

and high-temperature conditions in an aqueous or organic solvent.<sup>104</sup> Typically, TiO<sub>2</sub> precursors and gold precursors are mixed in a suitable solvent and sealed in a reactor, followed by heating at elevated temperatures for certain duration. This results in the formation of AuNPs anchored onto the TiO<sub>2</sub> surface.<sup>105</sup>

**Photodeposition method.** In this method, TiO<sub>2</sub> nanoparticles are dispersed in an aqueous solution containing a gold precursor. The suspension is then irradiated with UV light, which triggers the reduction of the gold precursor and deposition of AuNPs onto the TiO<sub>2</sub> surface due to the photoinduced electron transfer process.<sup>106</sup>

#### Ag/TiO<sub>2</sub> plasmonic NPs

tAg/TiO<sub>2</sub> nanophotocatalysts consist of silver (Ag) nanoparticles supported on titanium dioxide (TiO<sub>2</sub>) nanostructures. These nanocomposites exhibit enhanced photocatalytic activity and possess unique properties due to the synergistic effects between Ag and TiO<sub>2</sub>. The combination of Ag nanoparticles with TiO<sub>2</sub> nanostructures enhances the photocatalytic activity of TiO<sub>2</sub>, especially in the visible light region.<sup>107</sup> Ag nanoparticles act as plasmonic sensitizers, promoting visible light absorption and facilitating the generation of electron-hole pairs, which are crucial for photocatalytic reactions.<sup>108</sup> Ag nanoparticles exhibit surface plasmon resonance (SPR) properties, leading to enhanced light absorption and localized electromagnetic fields around the nanoparticles.<sup>109</sup> This SPR effect extends the absorption



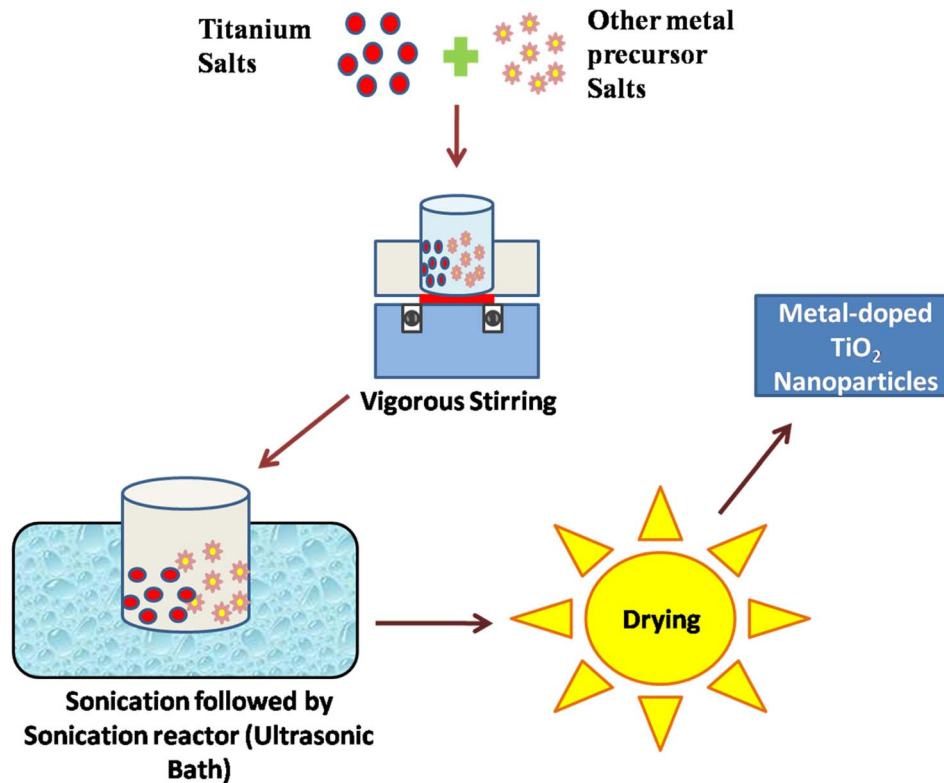


Fig. 10 Flow chart for the preparation of metal-doped  $\text{TiO}_2$  plasmonic nanoparticles via the sonochemical method.

spectrum of  $\text{TiO}_2$  into the visible region, thereby improving its photocatalytic efficiency.<sup>110</sup>  $\text{Ag}/\text{TiO}_2$  nanophotocatalysts exhibit antibacterial traits attributed to the emission of silver ions ( $\text{Ag}^+$ ) and the production of reactive oxygen species (ROS) under light exposure.<sup>111</sup> They are utilized for disinfection purposes in water treatment, air purification, and medical applications, effectively inhibiting the growth of bacteria and other pathogens.<sup>107</sup>  $\text{Ag}/\text{TiO}_2$  nanophotocatalysts are employed for the photocatalytic degradation of organic pollutants in water and air and pharmaceuticals. The synergistic effects between Ag nanoparticles and  $\text{TiO}_2$  nanostructures lead to the efficient generation of ROS, which degrade organic contaminants into harmless by-products under light irradiation.<sup>112</sup> To produce  $\text{H}_2$  fuel these nanophotocatalysts are utilized for photocatalytic water splitting. Ag nanoparticles promote the reduction of water molecules into  $\text{H}_2$  gas, while  $\text{TiO}_2$  facilitates water oxidation, leading to efficient  $\text{H}_2$  generation under light irradiation.<sup>113</sup>  $\text{Ag}/\text{TiO}_2$  nanophotocatalysts are used for environmental remediation due to their high photocatalytic activity, making them effective in treating various environmental pollutants.<sup>114</sup> Overall,  $\text{Ag}/\text{TiO}_2$  nanophotocatalysts offer versatile solutions for environmental remediation, energy conversion, and healthcare applications. Their unique properties and enhanced photocatalytic activity make them promising candidates for addressing various challenges in pollution control, renewable energy generation, and public health.

**Chemical reduction method.** This technique, akin to creating  $\text{Au}/\text{TiO}_2$  nanophotocatalysts, involves reducing silver ions onto the surface of  $\text{TiO}_2$  nanoparticles. A solution containing  $\text{TiO}_2$  nanoparticles is combined with a silver precursor solution (e.g., silver nitrate,  $\text{AgNO}_3$ ). Then, a reducing agent such as sodium borohydride ( $\text{NaBH}_4$ ), sodium citrate, or ethylene glycol is introduced to facilitate the reduction of silver ions into AgNPs on the  $\text{TiO}_2$  surface.<sup>115</sup>

**Photodeposition method.** In this approach,  $\text{TiO}_2$  nanoparticles are dispersed in a solution containing a silver precursor. The mixture is then exposed to UV light, triggering the reduction of the silver precursor and deposition of AgNPs onto the  $\text{TiO}_2$  surface through the photoinduced electron transfer process (ESI Fig. S2†).<sup>116</sup>

**Sol-gel method.** This method initiates with the hydrolysis and condensation of titanium alkoxides, leading to the formation of a  $\text{TiO}_2$  sol. Silver precursors can be integrated into the sol either directly or by saturating the  $\text{TiO}_2$  sol with a silver precursor solution. The resulting blend undergoes gelation and subsequent processing, including drying and calcination, to yield the  $\text{Ag}/\text{TiO}_2$  composite material<sup>117</sup> (ESI Fig. S3†).

**Hydrothermal/solvothermal method.** Performed under elevated temperature and pressure conditions in either an aqueous or organic solvent environment, this method involves mixing  $\text{TiO}_2$  precursors with silver precursors to synthesize  $\text{Ag}/\text{TiO}_2$  nanocomposites. This process facilitates the controlled growth of AgNPs on the  $\text{TiO}_2$  surface, resulting in a well-defined structure and enhanced photocatalytic activity.<sup>117</sup>



### Cu/TiO<sub>2</sub> plasmonic NPs

Cu/TiO<sub>2</sub> nanophotocatalysts consist of copper (Cu) nanoparticles doped into titanium dioxide (TiO<sub>2</sub>) nanostructures. These nanocomposites offer unique properties and find applications in various fields due to their enhanced photocatalytic activity and synergistic effects. Cu/TiO<sub>2</sub> nanophotocatalysts are extensively used for the photocatalytic degradation of organic pollutants in water and air, including pharmaceuticals, dyes and other harmful pollutants.<sup>118–120</sup> The presence of Cu nanoparticles enhances visible light absorption and promotes the generation of reactive oxygen species (ROS), such as superoxide radicals and hydroxyl radicals, which effectively degrade organic contaminants.<sup>121</sup> Cu/TiO<sub>2</sub> nanophotocatalysts are employed in photocatalytic water splitting to produce hydrogen (H<sub>2</sub>) fuel. Under light irradiation, TiO<sub>2</sub> facilitates water oxidation while Cu nanoparticles act as co-catalysts for the hydrogen evolution reaction, leading to efficient H<sub>2</sub> generation.<sup>122</sup> These nanophotocatalysts are utilized for the reduction of carbon dioxide (CO<sub>2</sub>) into value-added chemicals and fuels.<sup>123,124</sup> Cu nanoparticles serve as active sites for CO<sub>2</sub> adsorption and subsequent conversion into carbon monoxide (CO) or hydrocarbons under light irradiation, contributing to carbon capture and utilization strategies. Cu/TiO<sub>2</sub> nanophotocatalysts exhibit antibacterial properties due to the generation of ROS upon light irradiation. They are employed for disinfection purposes in water treatment, air purification, and medical applications, effectively killing bacteria and other pathogens.<sup>125</sup> Cu/TiO<sub>2</sub> nanophotocatalysts are integrated into photovoltaic devices or solar cells to enhance light absorption and improve energy conversion efficiency.<sup>126</sup> The synergistic effects between Cu nanoparticles and TiO<sub>2</sub> nanostructures enable efficient utilization of solar energy for various applications. However, Cu/TiO<sub>2</sub> nanophotocatalysts offer promising solutions for environmental remediation, energy conversion, and healthcare applications. Further research is ongoing to optimize their properties, enhance their stability, and explore new avenues for their utilization in emerging technologies.

**Sol-immobilisation method.** Nie *et al.* (2018) fabricated Cu–TiO<sub>2</sub> nanophotocatalysts by depositing copper onto TiO<sub>2</sub> (specifically, Evonik Aeroxide P25, comprising 80% anatase and 20% rutile phases) using a conventional sol immobilization method. Initially, an aqueous solution of polyvinyl alcohol was combined with Cu(NO<sub>3</sub>)<sub>2</sub>·3H<sub>2</sub>O, followed by the gradual addition of a freshly prepared NaBH<sub>4</sub> solution, leading to a color change indicating the formation of copper nanoparticles.<sup>127</sup> Subsequently, the TiO<sub>2</sub> support was added, and the mixture was stirred for 12 hours at 25 °C. Experiments were conducted in both ambient air and under an argon atmosphere. Samples were subjected to centrifugation, washed with distilled water, and then dried. These prepared samples were then utilized for subsequent catalytic and spectroscopic analyses.

**Photodeposition method.** Cu–TiO<sub>2</sub> photocatalysts were also synthesized using the photodeposition technique, where TiO<sub>2</sub> was combined with methanol and Ar was purged through suspension to eliminate residual O<sub>2</sub> from the reactor. Following this, illumination was initiated by using a Xe-lamp (Muller) for pre-reduction. Once the suspension's color changed to blue,

indicating the presence of titanium ions, an aqueous solution of Cu(NO<sub>3</sub>)<sub>2</sub>·3H<sub>2</sub>O was added dropwise and the mixture was then stirred at room temperature under an argon atmosphere. The resulting samples were subjected to centrifugation, washed and subsequently dried. The prepared samples were then employed for catalytic and characterization analyses.<sup>127</sup>

**Sol-gel method.** Nankya *et al.*, 2016, synthesized Cu–TiO<sub>2</sub> nanoparticles through the sol-gel approach. They used titanium oxysulfate as the TiO<sub>2</sub> precursor and copper trihydrate nitrate for doping. The procedure was conducted under normal atmospheric conditions. Firstly, the salts were dissolved in distilled water.<sup>128</sup> To maintain the pH, ammonium hydroxide was added. Afterwards, the solution was vigorously stirred and then aged for a certain period of time. Thereafter, the solution was filtered & dried, followed by calcination at 400–600 °C for few hours.

### Pt/TiO<sub>2</sub> plasmonic NPs

Pt/TiO<sub>2</sub> nanophotocatalysts consist of platinum (Pt) nanoparticles supported on titanium dioxide (TiO<sub>2</sub>) nanostructures. These nanocomposites exhibit enhanced photocatalytic activity and possess unique properties due to the synergistic effects between Pt and TiO<sub>2</sub>. Pt/TiO<sub>2</sub> nanophotocatalysts exhibit high photocatalytic activity, particularly in the degradation of organic pollutants and the production of hydrogen (H<sub>2</sub>) through water splitting. Pt nanoparticles act as co-catalysts, promoting charge separation and transfer at the TiO<sub>2</sub> surface and leading to enhanced electron–hole pair separation and reduced recombination rates, thereby enhancing the overall efficiency of photocatalytic reactions.<sup>129</sup> The presence of Pt nanoparticles on TiO<sub>2</sub> extends the absorption spectrum into the visible light region, allowing for enhanced utilization of solar energy in photocatalytic reactions.<sup>130</sup> Pt/TiO<sub>2</sub> nanophotocatalysts find diverse applications in environmental remediation, including the degradation of organic pollutants,<sup>131</sup> photocatalytic disinfection, and air purification.<sup>132</sup> Additionally, they are utilized in the synthesis of value-added chemicals from renewable feedstocks.<sup>133</sup> Overall, Pt/TiO<sub>2</sub> nanophotocatalysts offer promising solutions for addressing various challenges related to environmental pollution, renewable energy generation, and sustainable chemistry. Their unique properties and high photocatalytic activity make them valuable materials for a wide range of applications aimed at promoting environmental sustainability and advancing clean energy technologies (Table 2).

**Spray pyrolysis method.** The preparation of Pt–TiO<sub>2</sub> plasmonic nanoparticles was carried out in a flame spray pyrolysis

Table 2 Au and Ag distribution of different catalysts<sup>130</sup>

S. no.	Photocatalyst	Au species (%)			Ag species (%)	
		Au <sup>0</sup>	Au <sup>δ+</sup>	Au <sup>0</sup> /Au <sup>δ+</sup>	Ag <sup>0</sup>	Ag <sup>+</sup>
1	Ag/TiO <sub>2</sub>	—	—	—	66.5	33.5
2	Au/TiO <sub>2</sub>	87.4	12.6	6.93	—	—
3	Ag <sub>1</sub> –Au <sub>1</sub> /TiO <sub>2</sub>	81.8	18.2	4.49	62.0	38.0
4	Ag <sub>1</sub> –Au <sub>2</sub> /TiO <sub>2</sub>	79.4	20.6	3.85	62.8	37.2
5	Ag <sub>1</sub> –Au <sub>4</sub> /TiO <sub>2</sub>	78.8	21.2	3.82	60.7	39.3



reactor. Titanium and platinum precursors are dissolved in suitable solvents to form precursor solutions. These solutions typically contain titanium alkoxides (*e.g.*, titanium isopropoxide) and platinum salts (*e.g.*, platinum acetylacetonate). The precursor solutions are then atomized and introduced into a high-temperature flame using a carrier gas, such as oxygen or nitrogen. The flame serves as a reaction medium where the precursors undergo pyrolysis, subsequently leading to nanoparticle formation. The high temperatures in the flame lead to the decomposition and oxidation of the precursor compounds, resulting in the formation of Pt-TiO<sub>2</sub> nanoparticles.<sup>134</sup>

**Sol-gel method.** Titanium and platinum precursors are dissolved in solvents to create precursor solutions, typically containing titanium alkoxides like titanium isopropoxide and platinum salts such as chloroplatinic acid. Mixing these solutions initiates the sol-gel reaction, where hydrolysis of metal alkoxides forms metal hydroxides, followed by condensation reactions leading to the formation of a three-dimensional network structure. Controlled nucleation and growth within the gel matrix result in the formation of Pt-TiO<sub>2</sub> nanoparticles. Additional steps, like using a reducing agent or heat treatment, can aid in reducing metal ions to form metallic nanoparticles like Pt within the TiO<sub>2</sub> matrix. Gelation of the sol occurs gradually, converting it from liquid to solid, either spontaneously through polycondensation or by adjusting pH or temperature. Aging the gel further consolidates the nanoparticle structure and removes solvent molecules. Drying the aged gel removes the remaining solvent, forming a porous solid material. Calcination at high temperatures enhances crystallinity, eliminates organic residues, and induces desired phase transformations in Pt-TiO<sub>2</sub> nanoparticles.<sup>135</sup>

**Electron beam irradiation.** The synthesis of Pt-TiO<sub>2</sub> nanoparticles by electron beam irradiation involves exposing a mixture of titanium dioxide (TiO<sub>2</sub>) and platinum (Pt) precursors to an electron beam. This high-energy beam induces chemical reactions that result in the formation of Pt-TiO<sub>2</sub> nanoparticles. The process allows for precise control over nanoparticle size, composition, and distribution, offering advantages such as uniformity and reproducibility. Additionally, electron beam irradiation enables rapid synthesis at relatively low temperatures without the need for additional reducing agents or complex reaction conditions.<sup>136</sup>

**One-pot synthesis method.** The one-pot synthesis method for Pt-TiO<sub>2</sub> nanoparticles involves combining titanium III chloride (TiCl<sub>3</sub>) and platinum (platinic acid) precursors in a single reaction vessel. Through controlled chemical reactions occurring simultaneously in this single system, Pt-TiO<sub>2</sub> nanoparticles are formed.<sup>137</sup> This approach offers simplicity, efficiency, and the potential for precise control over nanoparticle properties, making it a versatile and convenient method for synthesizing Pt-TiO<sub>2</sub> nanoparticles with tailored characteristics for various applications.<sup>137</sup>

### Bimetal-doped TiO<sub>2</sub> plasmonic NPs

Bimetal-doped TiO<sub>2</sub> nanophotocatalysts incorporate two different metal dopants into the titanium dioxide nanostructure, enhancing photocatalytic activity and properties.<sup>138</sup> This doping improves charge separation, broadens light

absorption, and boosts the generation of reactive oxygen species, leading to more efficient pollutant degradation and hydrogen production.<sup>139</sup> Tunable bandgaps enable the absorption of a wider light spectrum, enhancing performance under UV and visible light.<sup>140</sup> Enhanced stability prolongs catalytic activity, while synergistic effects between dopants enhance performance *via* improved charge separation and reaction kinetics (Huang *et al.*, 2019).<sup>141</sup> Examples include Ag-Au/TiO<sub>2</sub>, Pt-Ni/TiO<sub>2</sub>, Fe-Cu/TiO<sub>2</sub> and Co-Ni/TiO<sub>2</sub> for pollutant degradation, hydrogen production, CO<sub>2</sub> reduction, pharmaceuticals degradation, and heavy metal removal. Various combinations cater to diverse environmental, energy, and healthcare applications, each offering unique benefits.<sup>142-144</sup>

According to Melvin *et al.*, 2015, the Pt-Au/TiO<sub>2</sub> nanocomposite, synthesized through a selective strategy, demonstrates enhanced hydrogen production without sacrificial agents.<sup>145</sup> Combining Au and Pt exploits their dual properties for plasmonic absorption and electron trapping, resulting in strong electronic interaction as confirmed by various analyses. The nanocomposite exhibits visible light activity and higher H<sub>2</sub> yield using pure water, paving the way for photocatalytic hydrogen production solely using natural resources. Rahul *et al.* (2018) found that incorporating Au-Pt bimetallic nanoparticles along with Ti<sup>3+</sup> doping within the TiO<sub>2</sub> nanophotocatalyst leads to outstanding solar photocatalytic performance.<sup>146</sup> The resulting Au-Pt/Ti<sup>3+</sup> nanocomposite TiO<sub>2</sub> catalyst exhibits a notably increased rate of hydrogen evolution. Furthermore, the conversion of this catalyst into a titania inverse opal photocatalyst (Au-Pt/Ti<sup>3+</sup>-TiO<sub>2</sub>) through colloidal photonic crystal (CPC) infiltration amplifies its solar hydrogen evolution capabilities, positioning it as a promising candidate for solar water splitting applications (ESI Fig. S4†).

**One-pot photo-deposition method.** Melvin *et al.* (2015) synthesized the bimetal (Au and Pt)-doped TiO<sub>2</sub> nanocomposite, involving several steps.<sup>145</sup> Initially, TiO<sub>2</sub> was dispersed in a mixture of water and solvents such as ethanol and methanol under continuous and vigorous stirring, followed by purging with argon gas. Auric chloride was then introduced into the mixture and the mixture was exposed to UV light for a specific duration.<sup>145</sup> Subsequently, a platinum-based salt was added, and the reaction mixture was subjected to prolonged UV exposure. After the photodeposition of the metal nanoclusters, the materials were washed with double-distilled water *via* centrifugation and were subsequently heated in an oven at an optimal temperature for a certain period to eliminate residual metal ions and methanol. Following these steps, the samples were tested for hydrogen production and underwent characterization.

**Co-precipitation method.** Ovcharov *et al.* (2020) prepared a solution containing a titanium precursor, such as titanium isopropoxide (TTIP), Ti(OBu)<sub>4</sub>, or titanium chloride and two different metal precursors, such as silver nitrate (AgNO<sub>3</sub>) and copper nitrate (Cu(NO<sub>3</sub>)<sub>2</sub>).<sup>147</sup> Then, the molar ratio of the metal precursors can be adjusted to achieve the desired doping concentration. Thereafter, a suitable solvent, such as ethanol or water is added to the solution while stirring the solution at room temperature or with mild heating to ensure homogeneity. Then, the pH of the solution is adjusted using a base, such as



Table 3 HMF conversion, product, yield and selectivity under visible light over different catalysts<sup>151</sup>

S. no.	Photocatalyst	HMF concentration (%)	Product	Yield (%)	Product selectivity (%)
1	Ag <sub>1</sub> -Au <sub>1</sub> /TiO <sub>2</sub>	29.4	FDCA	26.6	90.5
2	Ag <sub>1</sub> -Au <sub>2</sub> /TiO <sub>2</sub>	42.6	FDCA	41.8	98.1
3	Ag <sub>1</sub> -Au <sub>4</sub> /TiO <sub>2</sub>	33.4	FCCA	31.6	94.6
4	Au/TiO <sub>2</sub>	19.8	FDCA	16.9	85.4
5	Ag/TiO <sub>2</sub>	5.2	HMFCa	4.6	88.5
6	Au/TiO <sub>2</sub> & Ag/TiO <sub>2</sub> mixture	23.8	FDCA	21.4	89.9

ammonium hydroxide (NH<sub>4</sub>OH), to induce precipitation of metal-doped TiO<sub>2</sub> nanoparticles. With continuous stirring and aging, the solution allows for complete precipitation and formation of the doped TiO<sub>2</sub> nanoparticles (Sharma *et al.*, 2013).<sup>148</sup> Optionally, additional treatments such as calcination or hydrothermal treatment are performed to enhance crystallinity and photocatalytic activity. Finally, the bimetallic-doped TiO<sub>2</sub> nanoparticles are collected through centrifugation or filtration, and dried under vacuum or mild heating. This co-precipitation method allows for the simultaneous incorporation of two different metal dopants (Ag–Au, Cu–Ni, Pt–Au, Pt–Ni, *etc.*) into TiO<sub>2</sub> nanoparticles, resulting in bimetal-doped TiO<sub>2</sub> nanophotocatalysts with enhanced photocatalytic properties compared to pure TiO<sub>2</sub> (Sandoval *et al.*, 2013 & Sharma *et al.*, 2019).<sup>149,150</sup> The choice of metal dopants and their concentrations can be adjusted to optimize photocatalytic performance for specific applications.

Additionally, other synthesis methods such as sol–gel, hydrothermal (Tables 3 and 4), or impregnation methods can

also be adopted to incorporate bimetallic dopants into TiO<sub>2</sub> nanoparticles.<sup>151,152</sup>

## Applications of plasmonic nanomaterials in biomass-to-chemical and fuel conversion

Initially, the wood biomass undergoes pre-treatment followed by size reduction (where wood can convert into sawdust, pellets, *etc.*), and then treated with liquid hot water, dilute acid, steam explosion, and other solvents to remove dirt and impurities.<sup>153</sup> Plasmonic nanomaterials can be employed in biomass pretreatment processes to enhance the accessibility of cellulose and hemicellulose components. Through localized heating induced by plasmonic effects, these nanomaterials can promote the breakdown of lignin structures and improve the efficiency of subsequent enzymatic hydrolysis or chemical conversion processes.<sup>154</sup> Lignocellulosic biomass (cellulose, hemicellulose and lignin) can be obtained by acid hydrolysis, enzymatic hydrolysis, pyrolysis and gasification.<sup>151</sup>

Table 4 Plasmonic nanoparticles their synthesis and applications

Plasmonic nanoparticles	Synthesis method	Applications	References
Au/TiO <sub>2</sub>	Deposition–precipitation Sonochemical Impregnation Sol–gel Hydrothermal/ solvothermal Photodeposition	Dye-degradation, pollutant degradation, biomedical, drug degradation, hydrogen production, and production of valuable products	96, 99, 102, 104 and 106
Ag/TiO <sub>2</sub>	Chemical reduction Sol–gel Photodeposition Hydrothermal/ solvothermal	Dye-degradation, pollutant degradation, biomedical, drug degradation, hydrogen production, and production of valuable products	115 and 116
Bimetallic doped TiO <sub>2</sub>	One-pot deposition Co-precipitation Sol–gel Impregnation Hydrothermal	CO <sub>2</sub> reduction, pharmaceutical degradation, heavy metal degradation, environmental remediation, hydrogen production, and energy production	91 and 152
Cu/TiO <sub>2</sub>	Sol–gel Sol-immobilization Photodeposition	Heavy metal degradation, environmental remediation, hydrogen production, and energy production	127
Pt/TiO <sub>2</sub>	Spray pyrolysis Sol–gel Electron beam irradiation One-pot	Dye-degradation, pollutant degradation, biomedical, drug degradation, hydrogen production, and production of valuable products	134 and 136



## Applications of plasmonic photocatalysts in biomass conversion

The photocatalytic transformation of biomass into high-value chemicals and fuels stands out as one of the most dynamic fields in both scientific research and industry, driving sustainable development. From a chemical perspective, achieving the targeted production of desired products hinges on skillfully managing the interaction between radical oxidation species (activated by reactive oxygen species, ROS) and radical intermediates derived from the biomass substrate. Overcoming various technological challenges is essential for the practical application of these processes. This study aims to explore recent mechanistic strategies, focusing on optimizing ROS behaviour and designing materials/systems to enable selective biomass conversion.

The transformation of biomass into valuable compounds necessitates efficient methods capable of selectively breaking down biomass bonds or facilitating controlled upgrading of biomass-derived materials.<sup>155</sup> Within the realm of lignocellulose biorefineries, various processes such as alkaline or acid pretreatments, ozonolysis, hot water wet oxidation, and oxidative/reductive techniques are employed to separate lignin and polysaccharides.<sup>156,157</sup> This separation generates different product streams, with lignin serving as a significant source of aromatic compounds, driving extensive research into its valorization.<sup>158,159</sup> The selective oxidation of C=O and C–O bonds in lignin holds potential for producing valuable platform chemicals like benzene, toluene, xylene (BTX), as well as various phenolic monomers such as catechol, guaiacol, vanillin, syringaldehyde, and numerous acids.<sup>160</sup> Additionally, the oxidation of polysaccharides can yield diverse downstream products, such as 5-hydroxymethylfurfural (HMF), which can further be transformed into 2,5-furandicarboxylic acid (FDCA). HMF serves as a pivotal platform chemical with the potential for upgrading into various chemicals and fuels.<sup>161</sup> The conversion of lignocellulosic biomass (LCB) into valuable chemicals and fuels has been accomplished using biochemical, thermochemical, or microbial approaches, each presenting its advantages and drawbacks. Among these, thermocatalytic conversion stands out as a prominent method for LCB transformation.<sup>162,163</sup> Utilization of high reaction temperatures and pressures in this process often leads to the formation of unfunctionalized aromatics, alcohols, or alkanes.<sup>164</sup> Conversely, pyrolysis/gasification of LCB often yields syngas (CO and H<sub>2</sub>) and causes extensive bond cleavage, resulting in simplified aromatics and lower-value chemicals due to the removal of key functional groups from monomers.<sup>165</sup> These de-functionalized products may necessitate additional re-functionalization to obtain high-value chemicals, making the process atom-inefficient and energy-intensive. Given these challenges, recent focus in biomass research has shifted towards developing milder conversion strategies that can fully utilize biomass fractions (such as lignin and polysaccharides) to produce chemicals and fuels. Hydrogen is being explored as a clean and potentially renewable alternative to fossil fuels, leading to the investigation of photocatalysis as an eco-friendly LCB conversion route.<sup>166–168</sup> This approach is often referred to as “soft/mild radical oxidation” and is emerging as

a promising method for converting biomass while minimizing environmental impact.<sup>169,170</sup>

## Biomass conversion followed by reduction of HMF and furfural

Photocatalytic conversion of biomass components, hydrolysis of polysaccharides, and partial oxidation of biomass derivatives are key areas of focus, with potential applications in real-world settings.<sup>171</sup> The conversion of polysaccharides through photocatalysis has led to the production of various valuable products. Initially, the process involves the hydrolysis of  $\beta$ -1,4 glycosidic bonds within polysaccharides, breaking them down into monosaccharides or their intermediates (Fig. 11), which are then further oxidized to produce hydrogen (H<sub>2</sub>).<sup>172</sup> However, the use of water as a solvent for biomass-to-H<sub>2</sub> conversion is considered to be a challenging process because of strict pH requirements. A recent breakthrough introduced a one-pot strategy for the direct photo-reforming of cellulose, which is an innovative approach involving the use of sulphuric acid for cellulose hydrolysis at elevated temperatures over a platinumized TiO<sub>2</sub> photocatalyst under UV conditions.<sup>173</sup>

The simultaneous generation of electron donors facilitated biomass conversion to glucose, with these products also acting as electron donors with low oxidative power. To enhance the conversion of polysaccharides to essential monosaccharides and their derivatives, researchers have fine-tuned photocatalysts to induce a plasmonic thermal effect, boosting the hydrolysis process.<sup>172</sup> This advancement could streamline biomass conversion by eliminating separate pretreatment, hydrolysis, and chemical conversion steps. Under visible light conditions, significant cleavage of C–O–C  $\beta$ -1,4 glycosidic bonds in cellulose was achieved, yielding glucose and HMF.<sup>174</sup> A zeolite-based acid catalyst was used along with Au-nanoparticles (AuNPs) as the plasmonic photo-thermal catalyst, achieving notable yields at elevated temperatures over 16 hours. The mechanism involved localized surface plasmon resonance (LSPR) inducing acid proton formation, which facilitated glycosidic bond cleavage and subsequent glucose and HMF production. These advancements demonstrate the potential of photocatalysis in efficient biomass conversion, offering a pathway towards sustainable production of valuable chemicals and hydrogen. Continued research and optimization of photocatalytic processes will be instrumental in realizing the full potential of biomass-to-chemical conversion technologies (Fig. 12).<sup>174</sup>

## Plasmonic photocatalysts used for biomass to H<sub>2</sub> energy conversion

Photo-assisted water splitting for hydrogen production faces challenges such as low yields, expensive noble metal catalysts (Pt, Ir, Pd, and Ru), slow kinetics, and the need for hole scavengers.<sup>175</sup> Biomass, including sugars and lignocellulose, has been explored as hole scavengers to improve electron transfer for hydrogen generation, offering an alternative to fossil fuels.<sup>176</sup> Polysaccharide-based biomass conversion, utilizing glucose and xylose as hole scavengers, has shown promise for energy production.<sup>176,177</sup> For



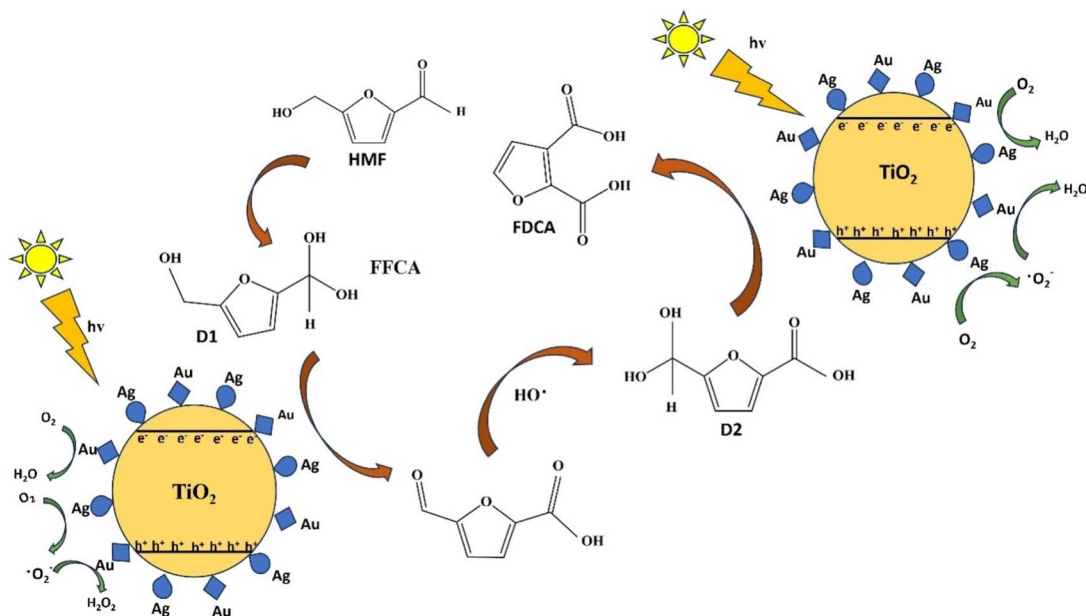


Fig. 11 Mechanism behind photocatalytic oxidation of HMF to FDCA using the Ag–Au/TiO<sub>2</sub> photocatalyst.

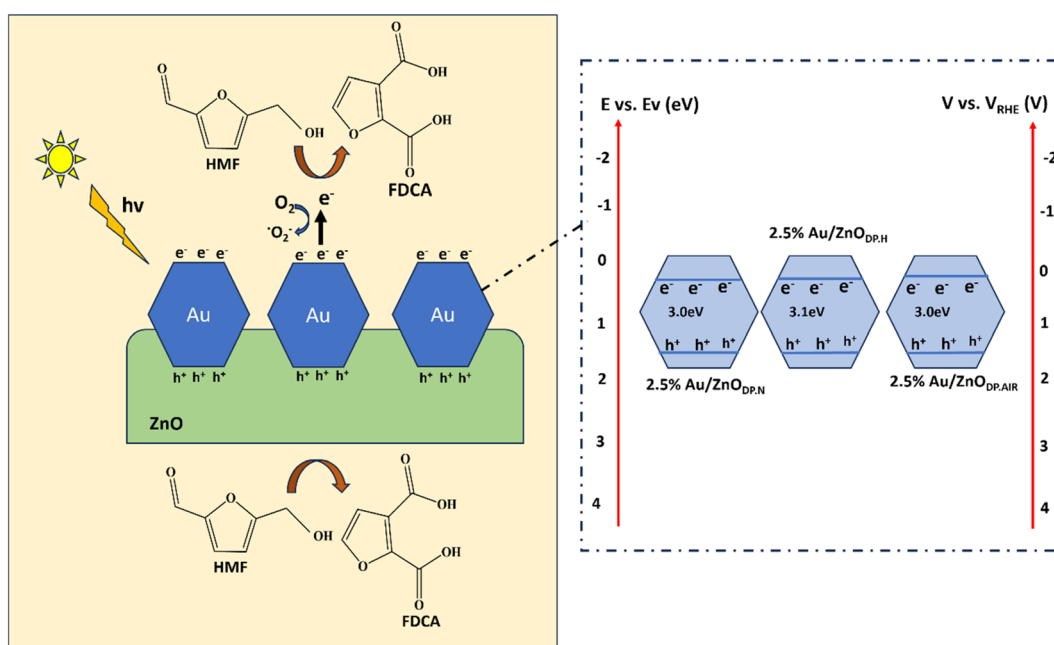


Fig. 12 Conversion of HMF to FDCA by photocatalytic oxidation.

example, using pine wood hydrolyzed products with TiO<sub>2</sub> yielded significant hydrogen (19.9 mL g<sub>substrate</sub><sup>-1</sup>), while glucose photoconversion to H<sub>2</sub> over Ru-doped LaFeO<sub>3</sub> resulted in high yields (910 μmol h<sup>-1</sup> g<sub>cat</sub><sup>-1</sup>).<sup>178</sup> Non-noble catalysts have emerged for simultaneous hydrogen and value-added chemical production, showcasing a dual strategy without the need for external electron donors.<sup>179</sup> These advancements highlight the potential for sustainable hydrogen production from biomass, signalling progress towards efficient and eco-friendly energy solutions.

## Photocatalysts used for CO<sub>2</sub> conversion to value-added products and fuels

### Plasmonic CO<sub>2</sub> reduction *via* DFT calculations

Using plasmonic silver (Ag) nanoparticles, Kumari *et al.* (2008) investigated the kinetics of visible light-driven CO<sub>2</sub> reduction with single nanoparticle spatial resolution.<sup>180</sup> They employed *in situ* surface-enhanced Raman spectroscopy (SERS) to observe



the adsorption of carbon dioxide ( $\text{CO}_2$ ) and the subsequent product formation, followed by Density Functional Theory (DFT) calculations to understand the mechanisms behind plasmonic activation leading to multi-electron reducing products and the reaction's selectivity.<sup>181</sup> A 514.5 nm laser was utilized in a gas-phase  $\text{CO}_2$  environment, with the counter half-reaction involving the oxidation of water deposited as  $-\text{OH}$  on the Ag surface under basic conditions. The study observed the stochastic emergence and disappearance of Raman peaks, which were attributed to various transitions and products (Fig. 13). DFT modelling revealed that  $\text{CO}_2$  is physisorbed on Ag, with subsequent activation occurring either through inter-band and intra-band reducing within Ag or through alterations in the highest occupied molecular orbital-lowest unoccupied molecular orbital (HOMO–LUMO) gap when  $\text{CO}_2$  is physically adsorbed on the Ag surface, leading to the formation of  $\text{CO}_2/\text{Ag}$  complexes (Fig. 14).<sup>182</sup> This activation mechanism involves energy transfer from localized surface plasmon resonance (LSPR) damping to activate the  $\text{CO}_2/\text{Ag}$  complex, resulting in electron transfer from Ag to  $\text{CO}_2$  and the generation of separated charges at the  $\text{CO}_2/\text{Ag}$  interface. The  $\text{CO}_2^{\cdot-}$  anion radicals further interact with  $\text{H}^+$  from water oxidation to generate intermediate species ( $\text{HOCO}^*$ ), which then transform into various products. The use of *in situ* single-nanoparticle SERS spectroscopy demonstrated the efficacy of detecting surface species ( $\text{HOCO}^*$ ) during  $\text{CO}_2$  reduction, providing valuable insights into plasmonic-mediated chemical processes and offering potential improvements for process efficiency.<sup>180</sup>

### Plasmon-assisted photothermal conversion for $\text{CO}_2$ reduction

The temperature plays a critical role in chemical reactions, influencing their rate and efficiency. Plasmonic nanoparticles

(NPs) can act as nanoheaters due to their ability to emit thermal energy, thereby accelerating nearby chemical reactions without the energy losses associated with traditional bulk heating methods. Sastre *et al.* (2019) explored the photothermal activation of chemical bonds using rod-like Ru catalysts supported on  $\gamma\text{-Al}_2\text{O}_3$  for  $\text{CO}_2$  methanation.<sup>183</sup> They developed a catalyst by impregnating  $\text{RuO}_2$  particles onto  $\gamma\text{-Al}_2\text{O}_3$ , achieving  $\text{CO}_2$  reduction under sunlight at 150 °C using hydrogen gas, with a conversion rate of about 55% to methane. The researchers observed an increase in methane production over multiple cycles, attributed to the reduction of  $\text{RuO}_2$  to metallic Ru in the presence of  $\text{H}_2$  at 150 °C. To confirm this reduction, they pre-reduced  $\text{RuO}_2$  with  $\text{H}_2$  at 250 °C, resulting in a catalyst that produced 1.6 times more methane.<sup>175</sup> Temperature monitoring with a thermocouple revealed that illumination increased the catalyst's temperature, impacting its kinetics. At low sunlight intensity and temperatures exceeding 189 °C, photoactivity was primarily due to heating effects, with similar activation energies observed under dark and light conditions at the same temperature. Non-thermal effects became significant at high catalyst temperatures, enhancing reaction rates under light compared to dark conditions.  $\text{CO}_2$  reduction without external heating produced methane at a rate of  $15.5 \text{ mmol}_{\text{CH}_4} \text{ g}_{\text{Ru}}^{-1} \text{ h}^{-1}$ , showing the catalyst's efficiency in utilizing light for reactions. The rod-shaped RuNPs exhibited stronger  $\text{CO}_2$  reduction capabilities than their spherical counterparts, attributed to their broader light absorption spectrum from different plasmon bands compared to the dipole plasmon mode of spherical NPs.<sup>181</sup> The study highlights the importance of catalyst morphology and optical properties in photothermal catalysis, with rod-shaped RuNPs showing superior performance due to their enhanced light absorption capabilities. These findings contribute to

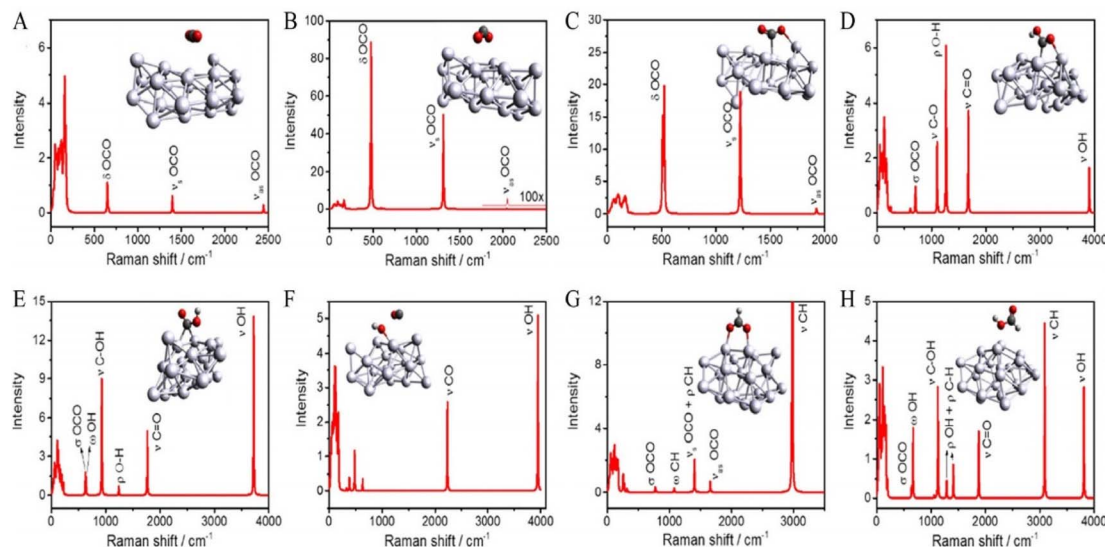


**Fig. 13** Raman spectra of various transitional compounds adsorbed on the surface of silver were calculated using Density Functional Theory (DFT). These compounds include: (A)  $\text{CO}_2$  molecules physisorbed on the surface, (B) negatively charged  $\text{CO}_2$  ( $\text{CO}_2^{\cdot-}$ ), (C)  $\text{CO}_2^{\cdot-}$  ions bonded to positively charged silver ions ( $\text{Ag}^{\delta+}$ ), (D)  $\text{HOCO}^*$  species, (E)  $\text{HOCO}^*$  species attached to the silver surface, (F) decomposition of  $\text{HOCO}^*$  resulting in surface-bound  $\text{CO}^*$  and  $\text{OH}^*$  on the silver surface, (G)  $\text{HCOO}^{\delta-}$  species linked to  $\text{Ag}^{\delta+}$ , and (H) adsorption of  $\text{HCOOH}$  on the silver surface. The color scheme denotes silver (Ag), oxygen (O) in red, carbon (C) in grey, and hydrogen (H) in white.<sup>181</sup>



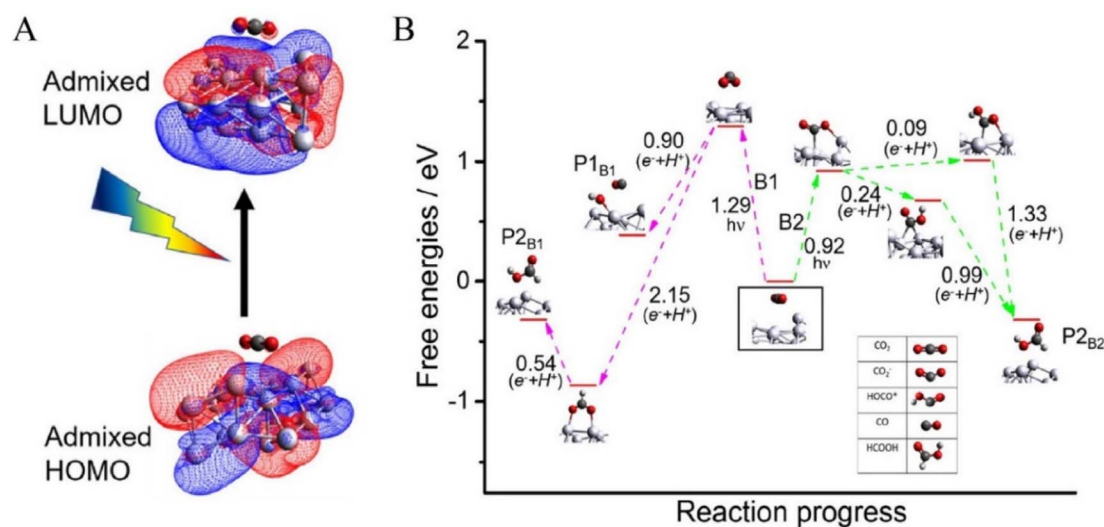


Fig. 14 The mechanism of photocatalytic CO<sub>2</sub> reduction, derived from Density Functional Theory (DFT) calculations, is outlined as follows: (A) examination of the Highest Occupied Molecular Orbital (HOMO) and Lowest Unoccupied Molecular Orbital (LUMO) of the CO<sub>2</sub>/Ag complex; (B) identification of potential reaction pathways.<sup>176</sup>

a better understanding of how plasmonic NPs can efficiently activate chemical reactions under light, paving the way for sustainable and energy-efficient catalytic processes.<sup>183</sup>

## Radical oxidation species: catalysts in photocatalytic transformations

Rather than relying on traditional homogeneous stoichiometric reductant/oxidant reagents, this heterogeneous photocatalytic process activates molecular oxygen, thereby providing redox capability to the medium. Consequently, it generates multiple reactive oxygen species (ROS), predominantly on the surface of the photocatalyst. Photocatalytic processes start with the light stimulation of the photocatalyst through exposure to light with an energy level comparable to or higher than the semiconductor photocatalyst's band gap, generating positive holes and electrons in the conduction and valence bands. Nevertheless, photoexcitation is not only consideration in photocatalytic systems but the rate of  $e^{-1}/h^{+}$  separation as well as the energy levels of the valence band (VB) and conduction band (CB) must be considered while evaluating the potential for ROS production by O<sub>2</sub> and H<sub>2</sub>O.<sup>184</sup> Photocatalytic redox processes for the oxidation or destruction of molecules in a medium depends on thermodynamic parameters.<sup>185</sup> For oxidation in a chemical medium, the energy level of the photocatalyst's valence band must be higher than that of the substrate, whereas, to achieve reduction, the energy level of the conduction band should exceed the potential of the substance that is being reduced. In photocatalytic ROS formation, the type and yield of produced ROS are determined by the photocatalyst used under the specified conditions.<sup>186</sup> Overall, the generation of ROS under different photocatalytic processes, include superoxide, conventional gas electrode, SHE, and one singlet oxygen.<sup>187</sup> The transformation of LCB to high-value compounds by

photogenerated reactive oxygen species is extremely complex and difficult. There is currently no solid data about the type of ROS required for selective LCB oxidation, and further experimental studies are needed to optimize the oxidative conditions to increase the yield of value-added compounds. Some research studies suggested that mildly oxidizing O<sub>2</sub><sup>-•</sup> might be more suitable for the photo-conversion of LCB than highly oxidizing HO<sup>•</sup>.<sup>187</sup> However, the origin and concentration of ROS are crucial factors to consider because they can alter the photo-conversion process. In simple terms, the photocatalytic oxidation action would differ depending on the type of LCB product. Due to the primary reactive oxygen species (ROS) activity, organic substrates undergo the formation of intermediate radical species, which are crucial in biomass conversions.<sup>188</sup> Notable radical intermediates formed on organic substrates include alkoxy radicals (RO<sup>•</sup>), hydrogen peroxide (RO<sub>2</sub>H), and peroxy radicals (RO<sub>2</sub><sup>•</sup>). These intermediates are generated as various sites within the feedstock are activated by ROS (Fig. 15).<sup>189</sup>

According to Verma *et al.* (2021), plasmonic photocatalysis utilizes localized surface plasmon resonance (LSPR) in nanoparticles (NPs) to concentrate light energy near their surfaces, generating excited charge carriers and heat.<sup>190</sup> This method enables novel and selective chemical reaction pathways not achievable with traditional thermal catalysis. The review delves into the fundamentals of plasmonic catalysis, focusing on CO<sub>2</sub> conversion to fuels and chemicals. It covers LSPR mechanisms, charge carrier generation, and various activation pathways on plasmonic nanocatalysts, emphasizing the role of charge carrier extraction in efficient catalysis. Multicomponent plasmonic catalysis combines plasmonic metals with active catalytic metals, overcoming the limitations of using metals like Pt and Pd in visible light photocatalysis.<sup>191</sup> The concept of "antenna-reactors" for synthesizing efficient photocatalysts is discussed, along with their applications in organic transformations and CO<sub>2</sub> conversion. Plasmonic catalysts, including "antenna-



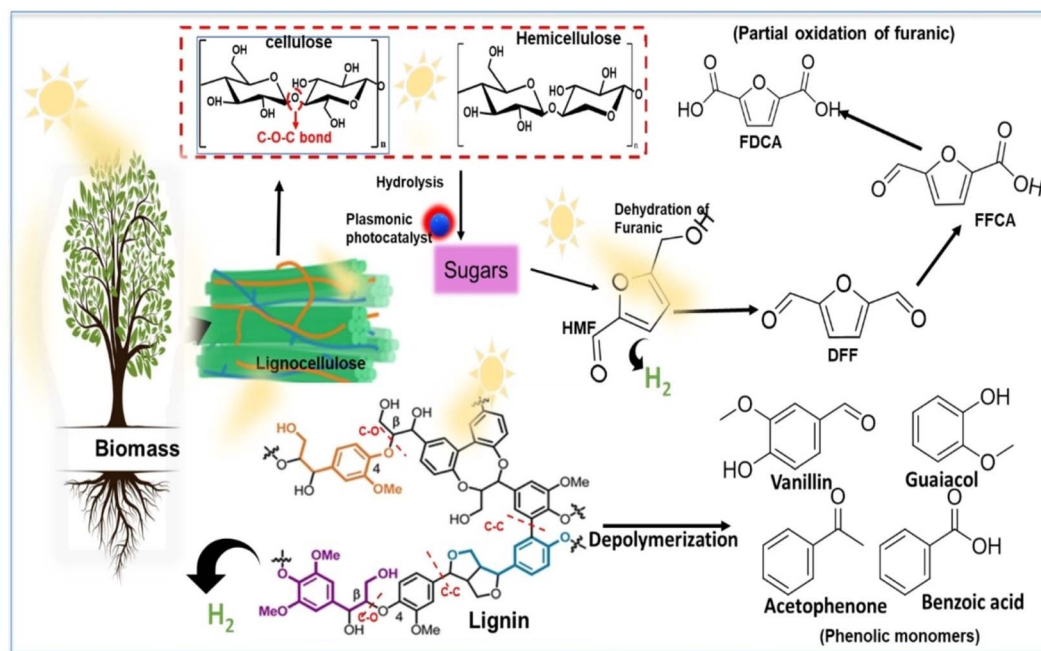


Fig. 15 Schematic diagram illustrating the pathways for photocatalytic conversion of lignocellulose biomass (LCB) into valuable chemicals and hydrogen gas. Key compounds involved in the process include 2,5-diformylfuran (DFF), 2,5-furandicarboxylic acid (FDCA), and 5-hydroxymethylfurfural (HMF).<sup>155</sup>

reactors,” demonstrate potential in generating hot charge carriers or providing heat for chemical reactions under light, enhancing photon absorption rates near nanocatalyst surfaces. They are also explored for low-temperature light-assisted catalytic processes like dry reforming of methane using CO<sub>2</sub>. Despite the advantages of selective product formation and lower activation energies compared to thermal catalysis, challenges such as high light energy input, low yields, and poor stability exist (Hu *et al.*, 2017).<sup>186</sup> Understanding complex reaction mechanisms through spectroscopy techniques and designing hybrid heterostructures are crucial for optimizing plasmonic catalysis. The field's growth holds promise in addressing energy and environmental issues by utilizing solar energy and CO<sub>2</sub>. However, further research is needed to enhance catalytic activity, selectivity, and stability in plasmonic photocatalysis, emphasizing the importance of material design strategies and *in situ* probing of plasmon-assisted reactions.<sup>183</sup>

## Conclusions and future prospects

In summary, the proliferation of studies in the past several years suggests that photocatalytic biomass conversion has a promising future. Improving the selectivity and effectiveness of photocatalysts, a better comprehension of biomass-based photo-conversion leading to more interesting processes and combinations, and the establishment of realistic purification processes for possible commercial production are all priorities. The continuous utilization of fossil fuels leading to increased levels of greenhouse gas (GHG) emissions, particularly CO<sub>2</sub>, has been identified as a major contributor to atmospheric pollution. One proposed solution to mitigate these emissions from various

decarbonized chemical processes involves recycling CO<sub>2</sub> into valuable bulk chemicals and fuels. This approach shows promise in addressing the issue. This review offers an overview of the thermocatalytic CO<sub>2</sub> hydrogenation reaction in the liquid phase, highlighting the potential use of both homogeneous and heterogeneous catalysts for commercializing this process.

Recent advancements in *in situ* characterization techniques and density functional theory (DFT) analysis have significantly enhanced our understanding of the various mechanistic pathways involved in CO<sub>2</sub> conversion. This improved understanding has led to the optimization of catalyst design, thereby increasing the yield and selectivity of liquid products.

Innovations such as the synthesis of plasmonic Ag and Au nanoparticles within wood substrates at low temperatures have been developed. This process results in structurally colored transparent wood, which not only acts as a green reducing agent but also serves as a scaffold for nanoparticles, ensuring their well-dispersed attachment to the substrate. The morphology of the substrate plays a crucial role in controlling the distribution of nanoparticles at the nanoscale, with nanoparticles forming both on and inside the wood cell walls, thereby creating an anisotropic wood structure of nanoparticles. The ongoing development of high-surface-area, thermally and mechanically robust, active, and selective plasmonic photocatalysts requires continued collaboration among researchers in catalysis, materials science, and chemical engineering.

This study involved the preparation of a semiconductor plasmonic photo-catalyst doped with noble metals through a simple deposition precipitation method. This catalyst was then utilized in the photo-catalytic oxidation of HMF to FDCA



under visible light. The improved efficiency of this process can be attributed to several factors:

- The presence of gold (Au) induces a Localized Surface Plasmon Resonance (LSPR) effect, which enhances the catalyst's absorption in the visible light spectrum and stimulates the generation of hot electrons.

- Treatment with hydrogen serves multiple purposes: it reduces the particle size of Au, strengthens the interaction between the metal and the support, and introduces more oxygen vacancies on the ZnO surface. These vacancies act as trapping sites for hot electrons, thereby enhancing the separation efficiency of electron-hole pairs.

- The Schottky barrier formed at the interface between Au and ZnO prevents the recombination of electron-hole pairs, thus prolonging their lifetime and facilitating the catalytic process.

- Through active species trapping experiments and radical-assisted Electron Spin Resonance (ESR) analysis, it was determined that superoxide radicals ( $O_2^{\cdot-}$ ) and positive holes ( $h^+$ ) are the active species responsible for the photocatalytic oxidation of HMF to FDCA.

In summary, there is promising evidence from recent studies regarding the potential of photocatalytic biomass conversion. It is imperative to continue advancing catalysts that offer improved selectivity and efficiency. Additionally, deeper insights into biomass-derived photoreactions are necessary, along with the exploration of new reaction pathways and catalyst combinations. Moreover, the development of viable purification methods is crucial for eventual industrial-scale production.

## Data availability

Data included as part of the article are available in the ESI.† Additional data are available upon reasonable request.

## Conflicts of interest

There are no conflicts to declare.

## References

- 1 A. Potbhare, P. Bhilkar, S. Yerpude, R. Madankar, S. Shingda, R. Adhikari and R. Chaudhary, *Appl. Emerg. Nanomater. Nanotechnol.*, 2023, vol. 148, pp. 304–333.
- 2 M. B. Tahir, I. Tahir, M. Rafique, M. S. Rafique, T. Nawaz and M. Sagir, *Nanotechnology and Photocatalysis for Environmental Applications*, Elsevier, 2020, pp. 65–76.
- 3 F. Lu and D. Astruc, *Coord. Chem. Rev.*, 2020, **408**, 213180.
- 4 A. Sharif, S. M. Khan, N. Gull, K. Rizwan, S. Munir, M. Shakeel, and A. Islam. *Nanomaterials in Biomass Conversion*. Woodhead Publishing, 2024, pp. 57–84.
- 5 X. Liu, S. Zhang, M. Wang and J. Wang, *Chin. Chem. Lett.*, 2024, **35**(3), 108723.
- 6 C. Rao, M. Xie, S. Liu, R. Chen, H. Su, L. Zhou, Y. Pang, H. Lou and X. Qiu, *ACS Appl. Mater. Interfaces*, 2021, **13**, 37.
- 7 F. Huang, *Materials for Biofuels*, *Mater. Energy*, 2014, **4**, 1–26.
- 8 S. Cheeseman, A. J. Christofferson, R. Kariuki, D. Cozzolino, T. Daeneke, R. J. Crawford, V. K. Truong, J. Chapman and A. Elbourne, *Adv. Sci.*, 2020, **7**, 1902913.
- 9 R. Chen, R. Li, L. Deitz, Y. Liu, R. J. Stevenson and W. Liao, *Biomass Bioenergy*, 2012, **39**, 128–138.
- 10 C. Chen, L. Wang, B. Zhu, Z. Zhou, S. I. El-Hout, J. Yang and J. Zhang, *J. Energy Chem.*, 2021, **54**, 528–554.
- 11 M. V. Galkin and J. S. M. Samec, *ChemSusChem*, 2016, **9**, 1544–1558.
- 12 C. Yang and X. Lü, *Advances in 2nd Generation of Bioethanol Production*, Woodhead Publishing, 2021, pp. 71–85.
- 13 J. C. Colmenares, A. Magdziarz and A. Bielejewska, *Bioresour. Technol.*, 2011, **102**, 11254–11257.
- 14 L. Wang, Z. Zhang, L. Zhang, S. Xue, W. O. S. Doherty, I. M. O'Hara and X. Ke, *RSC Adv.*, 2015, **5**, 85242–85247.
- 15 B. Zhou, J. Song, Z. Zhang, Z. Jiang, P. Zhang and B. Han, *Green Chem.*, 2017, **19**, 1075–1081.
- 16 D. A. Giannakoudakis, V. Nair, A. Khan, E. A. Deliyanni, J. C. Colmenares and K. S. Triantafyllidis, *Appl. Catal., B*, 2019, **256**, 117803.
- 17 A. Fujishima and K. Honda, *Nature*, 1972, **238**, 37–38.
- 18 Y. Meng, S. Yang and H. Li, *ChemSusChem*, 2022, **15**, 202102581.
- 19 T. Liu, J. Huang, J. Li, K. Wang, Z. Guo, H. Wu, S. Yang and H. Li, *Green Chem.*, 2023, **24**, 10338–10365.
- 20 M. Sajid, Y. Bai, D. Liu and X. Zhao, *Waste Biomass Valorization*, 2021, **12**, 3271–3286.
- 21 J. Li, T. Liu, N. Singh, Z. Huang, Y. Ding, J. Huang, P. Sudarsanam and H. Li, *Chem. Commun.*, 2023, **59**, 14341–14352.
- 22 D. Jose, C. M. Sorensen, S. S. Rayalu, K. M. Shrestha and K. J. Klabunde, *Int. J. Photoenergy*, 2013, 2013.
- 23 M. Bellardita, V. Loddo and L. Palmisano, *Mini-Rev. Org. Chem.*, 2020, **17**, 884–901.
- 24 N. Srivastava, R. Singh, M. Srivastava, A. Mohammad, S. Harakeh, R. P. Singh, D. B. Pal, S. Haque, H. H. Tayeb, M. Moulay and V. K. Gupta, *Bioresour. Technol.*, 2023, **369**, 128471.
- 25 B. Zhang, J. Li, L. Guo, Z. Chen and C. Li, *Appl. Catal., B*, 2018, **237**, 660–664.
- 26 H. Hao, L. Zhang, W. Wang and S. Zeng, *ChemSusChem*, 2018, **11**, 2810–2817.
- 27 L. Zhang, W. Wang, S. Zeng, Y. Su and H. Hao, *Green Chem.*, 2018, **20**, 3008–3013.
- 28 K. Gupta and T. S. Chundawat, *Biomass Bioenergy*, 2020, **143**, 105840.
- 29 M. B. Tahir, M. Sohaib, M. Sagir and M. Rafique, *Encyclopedia of Smart Materials*, Elsevier, 2022, p. 578.
- 30 A. Y. Ibrahim, A. Tawfik, A. S. El-Dissouky, T. Kassem, N. S. Alhajeri and D. Pant, *Bioresour. Technol.*, 2022, **361**, 127614.
- 31 S. Tedesco, G. Hurst, A. Imtiaz, M. Ratova, L. Tosheva and P. Kelly, *Energy*, 2020, 117954.
- 32 M. Singhvi and B. S. Kim, *Bioresour. Technol.*, 2022, **365**, 128108.



- 33 I. A. Sanusi, T. N. Suinyuy and G. E. B. Kana, *Biotechnol. Rep.*, 2021, **29**, e00585.
- 34 M. Yasuda, A. Miura, R. Yuki, Y. Nakamura, T. Shiragami, Y. Ishii, *et al.*, *J. Photochem. Photobiol., A*, 2011, **220**, 195–199.
- 35 R. Prado, X. Erdocia and J. Labidi, *Chemosphere*, 2013, **91**, 1355–1361.
- 36 J. Gong, A. Imbault and R. Farnood, *Appl. Catal., B*, 2017, **204**, 296–303.
- 37 G. Han, Y. H. Jin, R. A. Burgess, N. E. Dickenson, X. M. Cao and Y. Sun, *J. Am. Chem. Soc.*, 2017, **139**, 15584–15587.
- 38 M. Antar, D. Lyu, M. Nazari, A. Shah, X. Zhou and D. L. Smith, *Renewable Sustainable Energy Rev.*, 2021, **139**, 110691.
- 39 W. Zegada-Lizarazu, J. L. N. Carvalho, A. Parenti, S. Tenelli, C. M. Sastre, P. Ciria, C. Myrsini, E. Alexopoulou, A. Bonomi and A. Monti, *Biomass Bioenergy*, 2011, **35**, 12–25.
- 40 R. Dominik and R. Janssen, *The Biogas Handbook: Science, Production and Applications*, IEA Bioenergy, 2013, p. 19.
- 41 K. Chojnacka, P. P. Wiczorek, G. Schroeder and I. Michalak, *Algae biomass: Characteristics and applications: Towards algae-based products*, *Dev. Appl. Phycol.*, 2018, vol. 8.
- 42 S. K. R. Namasivayam, P. Prakash, V. Babu, E. J. Paul, R. S. A. Bharani, J. A. Kumar, M. Kavisri and M. Moovendhan, *J. Cleaner Prod.*, 2023, 136386.
- 43 B. Bharathiraja, M. Chakravarthy, R. R. Kumar, D. Yogendran, D. Yuvaraj, J. Jayamuthunagai, R. P. Kumar and S. Palan, *Renewable Sustainable Energy Rev.*, 2015, **47**, 634–653.
- 44 Y. Li, L. W. Zhou and R. Z. Wang, *Renewable Sustainable Energy Rev.*, 2017, **80**, 1017–1030.
- 45 B. D. Titus, K. Brown, H. S. Helmisaari, E. Vanguelova, I. Stupak, A. Evans, N. Clarke, C. Guidi, V. J. Bruckman, K. I. Varnagiryte and K. Armolaitis, *Energy Sustainability Soc.*, 2021, **11**, 1–32.
- 46 M. Danish and T. Ahmad, *Renewable Sustainable Energy Rev.*, 2018, **87**, 1–21.
- 47 X. Zhang, Y. Weihong and W. Blasiak, *Energy Fuels*, 2011, **25**, 4786–4795.
- 48 X. Si, F. Lu, J. Chen, R. Lu, Q. Huang, H. Jiang, E. Taarning and J. Xu, *Green Chem.*, 2017, **19**, 4849–4857.
- 49 B. C. Saha, *J. Ind. Microbiol. Biotechnol.*, 2003, **30**, 279–291.
- 50 H. Barsett, A. Ebringerová, S. E. Harding, T. Heinze, Z. Hromádková, C. Muzzarelli, R. A. A. Muzzarelli, B. S. Paulsen and O. A. El Seoud, *J. Am. Chem. Soc.*, 2005, 689–696.
- 51 M. F. Qaseem, H. Shaheen and A. M. Wu, *Renewable Sustainable Energy Rev.*, 2011, **144**, 110996.
- 52 P. Maijala, *Heterobasidionannosum and Wood Decay: Enzymology of Cellulose, Hemicellulose, and Lignin Degradation*, 2000.
- 53 A. Demirbaş, *Energy Sources*, 2005, **27**, 761–767.
- 54 R. B. Santos, W. H. Peter, H. Jameel and H. Chang, *Bioresource*, 2013, **8**, 23–31.
- 55 S. Liu, H. Lu, R. Hu, A. Shupe, L. Lin and B. Liang, *Biotechnol. Adv.*, 2012, **30**, 785–810.
- 56 L. L. Dilworth, C. K. Riley and D. K. Stennett, *Pharmacognosy*, Academic Press, 2024, 49–74.
- 57 N. Guessan, J. L. Lepetit, B. F. Niamké, N. ' J. C. Yao and N. Amusant, *For. Prod. J.*, 2023, **73**, 194–208.
- 58 J. Custódio, J. Broughton and H. Cruz, *Int. J. Adhes. Adhes.*, 2009, **29**, 173–185.
- 59 M. Dunky, *Handbook of Adhesive Technology*, CRC Press, 2017, pp. 511–574.
- 60 D. Suteu, C. Zaharia, C. Popovici, T. Malutan, L. Rusu and L. Tabacaru, *Environ. Eng. Manage. J.*, 2016, **15**, 3.
- 61 A. R. Bodie, A. C. Micciche, G. G. Atungulu, M. J. Rothrock Jr and S. C. Ricke, *Front. Sustainable Food Syst.*, 2019, **3**, 47.
- 62 I. Glushankova, A. Ketov, M. Krasnovskikh, L. Rudakova and I. Vaisman, *Resources*, 2018, **7**, 31.
- 63 O. C. Okeh, C. O. Onwosi and F. J. C. Odibo, *Renewable Energy*, 2014, **62**, 204–208.
- 64 S. Nanda, A. K. Dalai, F. Berruti and J. A. Kozinski, *Waste Biomass Valorization*, 2016, **7**, 201–235.
- 65 S. Wang, H. Li, S. Zou and G. Zhang, *Energy Build.*, 2020, **226**, 110358.
- 66 S. K. S. Hossain, L. Mathur and P. K. Roy, *J. Asian Ceram. Soc.*, 2018, **6**, 299–313.
- 67 N. Nurhidayati and M. Mariati, *J. Degraded Min. Lands Manage.*, 2014, **2**, 223.
- 68 M. H. Shaw, J. Twilton and D. W. C. MacMillan, *J. Org. Chem.*, 2016, **81**, 6898–6926.
- 69 S. Zhu, Q. Meng, L. Wang, J. Zhang, Y. Song, H. Jin, K. Zhang, H. Sun, H. Wang and B. Yang, *Angew. Chem., Int. Ed.*, 2013, **52**, 3953–3957.
- 70 J. Matos, C. Nahas, L. Rojas and M. Rosales, *J. Hazard. Mater.*, 2011, **196**, 360–369.
- 71 R. Spinelli, L. Eliasson and H. S. Han, *Curr. For. Rep*, 2020, **6**, 210–219.
- 72 C. A. Hankin, B. Stokes and A. N. D. A. Twaddle, *Biomass Bioenergy*, 1995, **9**, 191–203.
- 73 B. C. Vidal, B. S. Dien, K. C. Ting and V. Singh, *Appl. Biochem. Biotechnol.*, 2011, **164**, 1405–1421.
- 74 P. Perre and R. B. Keey, *Handbook of Industrial Drying*, CRC Press, 2014, pp. 822–872.
- 75 J. S. Tumuluru, C. T. Wright, J. R. Hess and K. L. Kenney, *Biofuels, Bioprod. Biorefin.*, 2011, **5**, 683–707.
- 76 V. B. Agbor, N. Cicek, R. Sparling, A. Berlin and D. B. Levin, *Biotechnol. Adv.*, 2011, **29**, 675–685.
- 77 C. Lokmit, K. Nakason, S. Kuboon, A. Jiratanachotikul and B. Panyapinyopol, *Biomass Convers. Biorefin.*, 2022, 1–13.
- 78 H. S. Kambo and A. Dutta, *Energy Convers. Manage.*, 2015, **105**, 746–755.
- 79 Z. Luan, T. Chen and L. Zhang, *IOP Conf. Ser.: Mater. Sci. Eng.*, 2020, **603**, 012002.
- 80 C. Y. Tsai, H. G. Im and T. Y. Kim, *Int. Mech. Eng. Congr. Expo.*, 2007, **43025**, 537–545.
- 81 L. Lin and M. Strand, *Appl. Energy*, 2013, **109**, 220–228.
- 82 A. Rani, R. Reddy, U. Sharma, P. Mukherjee, P. Mishra, A. Kuila, L. C. Sim and P. Saravanan, *J. Nanostruct. Chem.*, 2018, **8**, 255–291.
- 83 H. Tong, S. Ouyang, Y. Bi, N. Umezawa, M. Oshikiri and J. Ye, *Adv. Mater.*, 2012, **24**, 229–251.



- 84 Y. Sang, H. Liu and A. Umar, *ChemCatChem*, 2015, **7**, 559–573.
- 85 H. Wang, W. Liu, X. He, P. Zhang, X. Zhang and Y. Xie, *J. Am. Chem. Soc.*, 2020, **142**, 14007–14022.
- 86 S. G. Kumar and K. S. R. K. Rao, *Appl. Surf. Sci.*, 2017, **391**, 124–148.
- 87 N. D. Cuong and D. T. Quang, *Vietnam J. Chem.*, 2020, **58**, 434–463.
- 88 N. Sharma, H. Ojha, A. Bharadwaj, D. P. Pathak and R. K. Sharma, *RSC Adv.*, 2015, **5**, 53381–53403.
- 89 W. Shang, Y. Li, H. Huang, F. Lai, M. B. J. Roefsaers and B. Weng, *ACS Catal.*, 2021, **11**, 4613–4632.
- 90 J. H. Bang and P. V. Kamat, *ACS Nano*, 2009, **3**, 1467–1476.
- 91 W. He, H. Jia, J. Cai, X. Han, Z. Zheng, W. G. Wamer and J. J. Yin, *J. Phys. Chem. C*, 2016, **120**, 3187–3195.
- 92 B. Ran, L. Ran, Z. Wang, J. Liao, D. Li, K. Chen, W. Cai, J. Hou and X. Peng, *Chem. Rev.*, 2023, **123**, 12371–12430.
- 93 L. Bai, M. Wei, E. Hong, D. Shan, L. Liu, W. Yang, X. Tang and B. Wang, *Mater. Chem. Phys.*, 2020, **246**, 122825.
- 94 S. Fooladi, M. H. Nematollahi and S. Irvani, *Environ. Res.*, 2023, 116287.
- 95 W. K. Darkwah and K. A. Oswald, *Nanoscale Res. Lett.*, 2019, **14**, 1–17.
- 96 B. Kholikov, J. Hussain, S. Hayat and H. Zeng, *J. Chin. Chem. Soc.*, 2021, **68**, 1908–1915.
- 97 D. Huang, M. Wen, C. Zhou, Z. Li, M. Cheng, S. Chen, W. Xue, L. Lei, Y. Yang, W. Xiong and W. Wang, *Appl. Catal., B*, 2020, **267**, 118651.
- 98 S. Veziroglu, A. L. Obermann, M. Ullrich, M. Hussain, M. Kamp, L. Kienle, T. Leifßner, H. G. Rubahn, O. Polonskyi, T. Strunskus and J. Fiutowski, *ACS Appl. Mater. Interfaces*, 2020, **12**, 14983–14992.
- 99 B. Gupta, A. A. Melvin, T. Matthews, S. Dash and A. K. Tyagi, *Renewable Sustainable Energy Rev.*, 2016, **58**, 1366–1375.
- 100 Y. Mizukoshi, S. Seino, T. Kinoshita, T. Nakagawa, T. A. Yamamoto and S. Tanabe, *Scr. Mater.*, 2006, **54**, 609–613.
- 101 Y. Mizukoshi, S. Satoshi, K. Okitsu, T. Kinoshita, Y. Otome, T. Nakagawa and T. A. Yamamoto, *Ultrason. Sonochem.*, 2005, **12**, 191–195.
- 102 C. Rodríguez-Martínez, A. E. García-Domínguez, F. Guerrero-Robles, R. Omar Saavedra-Díaz, G. Torres-Torres, C. Felipe, R. Ojeda-López, A. Silahua-Pavón and A. Cervantes-Urbe, *J. Compos. Sci.*, 2020, **4**, 89.
- 103 D. Crişan, N. Drăgan, M. Răileanu, M. Crişan, A. Ianculescu, D. Luca, A. Năstuță and D. Mardare, *Appl. Surf. Sci.*, 2011, **257**, 4227–4231.
- 104 N. B. Saber, A. Mezni, A. Alrooqi and T. Altalhi, *Mater. Res. Express*, 2021, **8**, 045016.
- 105 Y. Gu, C. Li, J. Bai, J. Wang and T. Ma, *Vacuum*, 2016, **130**, 1–6.
- 106 A. Tanaka, S. Sakaguchi, K. Hashimoto and H. Kominami, *Catal. Sci. Technol.*, 2014, **4**, 1931–1938.
- 107 J. Singh, N. Tripathi and S. Mohapatra, *Nano-Struct. Nano-Objects*, 2019, **18**, 100266.
- 108 P. Wang, B. Huang, Y. Dai and M.-H. Whangbo, *J. Phys. Chem. C*, 2012, **114**, 9813–9825.
- 109 K. Khurana and N. Jaggi, *Plasmonics*, 2021, **14**, 981–999.
- 110 X. Yang, Y. Wang, L. Zhang, H. Fu, P. He, D. Han, T. Lawson and X. An, *Catalysts*, 2020, **10**, 139.
- 111 S. P. Deshmukh, S. M. Patil, S. B. Mullani and S. D. Delekar, *Mater. Sci. Eng., C*, 2019, **97**, 954–965.
- 112 P. Sanitnon, S. Chiarakorn, C. Chawengkijwanich, S. Chuangchote and T. Pongprayoon, *J. Aust. Ceram. Soc.*, 2020, **56**, 579–590.
- 113 N. L. Reddy, V. N. Rao, M. Vijayakumar, R. Santhosh, S. Anandan, M. Karthik, M. V. Shankar, K. R. Reddy, N. P. Shetti, M. N. Nadagouda and T. M. Aminabhavi, *Int. J. Hydrogen Energy*, 2019, **44**, 10453–10472.
- 114 R. Frankowski, A. Zgoła-Grześkowiak, T. Grześkowiak, E. Stanisz, J. Werner and J. Platkiewicz, *Processes*, 2022, **10**, 2523.
- 115 L. Somlyai-Sipos, P. Baumli, A. Sycheva, G. Kaptay, E. Szőri-Dorogházi, F. Kristály, T. Mikó and D. Janovszky, *Appl. Surf. Sci.*, 2020, **533**, 147494.
- 116 S. C. Chan and M. A. Barteau, *Langmuir*, 2005, **21**, 5588–5595.
- 117 R. Estévez, E. Patricio, J. L. Lago and S. P. Thirumuruganandham, *Materials*, 2023, **16**, 3076.
- 118 N. Riaz, M. A. Bustam, F. K. Chong, Z. B. Man, M. S. Khan and A. M. Shariff, *Sci. World J.*, 2014, 342020.
- 119 M. Hadei, A. Mesdaghinia, R. Nabizadeh, A. H. Mahvi, S. Rabbani and K. Naddafi, *Environ. Sci. Pollut. Res.*, 2021, **28**, 13055–13071.
- 120 A. S. Ethiraj, D. S. Rhen, A. V. Soldatov, G. A. M. Ali and Z. H. Bakr, *Int. J. Thin Film Sci. Technol.*, 2021, **10**, 169–182.
- 121 Z. Yang, D. Dai, Y. Yao, L. Chen, Q. Liu and L. Luo, *J. Chem. Eng.*, 2017, **322**, 546–555.
- 122 M. Rafique, S. Hajra, M. Irshad, M. Usman, M. Imran, M. A. Assiri and W. M. Ashraf, *ACS Omega*, 2023, **8**, 25640–25648.
- 123 F. O. Ochedi, D. Liu, J. Yu, A. Hussain and Y. Liu, *Environ. Chem. Lett.*, 2021, **19**, 941–967.
- 124 M. B. Tahir and K. N. Riaz, *Nanomaterials and Photocatalysis in Chemistry*, Springer Singapore, 2021.
- 125 M. Ikram, E. Umar, A. Raza, A. Haider, S. Naz, A. Ul-Hamid, J. Haider, I. Shahzadi, J. Hassan and S. Ali, *RSC Adv.*, 2020, **10**, 24215–24233.
- 126 A. Ashok, R. J. Beula, R. Magesh, G. Unnikrishnan, P. M. Paul, H. C. Bennett, F. Joselin and A. Abiram, *Opt. Mater.*, 2024, **148**, 114896.
- 127 J. Nie, A. O. T. Patrocínio, S. Hamid, F. Sieland, J. Sann, S. Xia, D. W. Bahnemann and J. Schneider, *Phys. Chem. Chem. Phys.*, 2018, **20**, 5264–5273.
- 128 R. Nankya and K. Kim, *J. Nanosci. Nanotechnol.*, 2016, **16**, 11631–11634.
- 129 X. Lin and J. Wang, *Int. J. Hydrogen Energy*, 2019, **44**, 31853–31859.
- 130 Z. Zhang, Z. Wang, S. Cao and C. Xue, *J. Phys. Chem. C*, 2013, **117**, 25939–25947.
- 131 K. Alamelu and J. Ali, *J. Environ. Chem. Eng.*, 2018, **6**, 5720–5731.
- 132 P. Ciambelli, V. Vaiano and D. Sannino, Nanotechnology in Catalysis: Applications in the Chemical Industry, *Energy*



- Development, and Environment Protection*, Wiley, 2017, pp. 873–890.
- 133 J. C. C. Quintero, *Producing Fuels and Fine Chemicals from Biomass Using Nanomaterials*, CRC Press, 2013, vol. 5, p. 283.
- 134 W. Y. Teoh, L. Mädler, D. Beydoun, S. E. Pratsinis and R. Amal, *Chem. Eng. Sci.*, 2005, **60**, 5852–5861.
- 135 F. Chekin, S. Bagheri and S. B. A. Hamid, *Sens. Actuators, B*, 2013, **177**, 898–903.
- 136 S. Kageyama, Y. Sugano, Y. Hamaguchi, J. Kugai, Y. Ohkubo, S. Seino, T. Nakagawa, S. Ichikawa and A. Takao, *Mater. Res. Bull.*, 2013, **48**, 1347–1351.
- 137 S. Cho, G. Yim, J. Koh, H. Jang and J. T. Park, *Mater. Today Chem.*, 2023, **32**, 101644.
- 138 X. H. Tai, C. W. Lai, J. C. Juan and K. M. Lee, *Nanomaterials for Air Remediation*, Elsevier, 2020, pp. 151–165.
- 139 L. Hu, Y. Liao, D. Xia, F. Peng, L. Tan, S. Hu, C. Zheng, X. Lu, C. He and D. Shu, *J. Chem. Eng.*, 2020, **385**, 123824.
- 140 W. He, H. Jia, J. Cai, X. Han, Z. Zheng, W. G. Wamer and J. Yin, *J. Phys. Chem. C*, 2016, **120**, 3187–3195.
- 141 J. Huang, Y. Wang, X. Liu, Y. Li, X. Hu, B. He, Z. Shu, Z. Li and Y. Zhao, *Nano Energy*, 2019, **59**, 33–40.
- 142 E. Grabowska, M. Marchelek, T. Klimczuk and W. Lisowski, *J. Mol. Catal. A: Chem.*, 2016, **424**, 241–253.
- 143 A. Monga, A. Bathla and B. Pal, *Sol. Energy*, 2017, **155**, 1403–1410.
- 144 A. Zielinska-Jurek and J. Hupka, *J. Nanomater.*, 2014, **3**.
- 145 A. A. Melvin, K. Illath, T. Das, T. Raja, S. Bhattacharyya and C. S. Gopinath, *Nanoscale*, 2015, **7**, 13477–13488.
- 146 T. K. Rahul, M. Mohan and N. Sandhyarani, *ACS Sustain. Chem. Eng.*, 2018, **6**, 3049–3059.
- 147 M. L. Ovcharov, A. M. Mishura, E. A. Mikhalyova and G. Vasylym, *Mater. Sci. Semicond. Process.*, 2020, **111**, 104985.
- 148 P. K. Sharma, N. Saxena, A. Bhatt, C. Rajagopal and P. K. Roy, *Catal. Sci. Technol.*, 2013, **3**, 1017–1026.
- 149 A. Sandoval, C. Louis and R. Zanella, *Appl. Catal., B*, 2013, **140**, 363–377.
- 150 G. Sharma, A. Kumar, S. Sharma, M. Naushad, R. P. Dwivedi and A. Zeid, *J. King Saud Univ., Sci.*, 2019, **31**, 257–269.
- 151 X. Zhang, M. Tu and M. G. Paice, *Bioenergy Res.*, 2011, **44**, 246–257.
- 152 R. Estévez, E. Patricio, J. López Lago and S. P. Thirumuruganandham, *Materials*, 2023, **16**, 3076.
- 153 B. C. Saha, *Lignocellulose Biodegradation and Applications in Biotechnology*, ACS Publication, 2004.
- 154 U. D. S. Zaheer, S. Bajar, A. Devi, P. K. Rose, M. Suhag, A. Yadav, D. K. Yadav, T. Deswal, J. Kaur, R. Kothari, D. Pathania, N. Rani and A. Singh, *Enzyme Microb. Technol.*, 2023, 110304.
- 155 D. Aboagye, R. Djellabi, F. Medina and S. Contreras, *Angew. Chem.*, 2023, **135**, e202301909.
- 156 L. A. Z. Torres, A. L. Woiciechowski, V. O. A. de Tanobe, S. G. Karp, L. C. G. Lorenci, C. Faulds and C. R. Soccol, *J. Cleaner Prod.*, 2020, **263**, 121499.
- 157 *Horizons in Bioprocess Engineering*, ed. R. Pogaku, Springer International Publishing, 2019.
- 158 P. Gallezot, *Chem. Soc. Rev.*, 2012, **41**, 1538–1558.
- 159 C. O. Tuck, E. Pérez, I. T. Horváth, R. A. Sheldon and M. Poliakoff, *Science*, 2012, **337**, 695–699.
- 160 C. Liu, S. Wu, H. Zhang and R. Xiao, *Fuel Process. Technol.*, 2019, **191**, 181–201.
- 161 J. J. Bozell and G. R. Petersen, *Green Chem.*, 2010, **12**, 539–554.
- 162 M. I. Alam, S. De, T. S. Khan, M. A. Haider and B. Saha, *Ind. Crops Prod.*, 2018, **123**, 629–637.
- 163 C. Chen, L. Wang, B. Zhu, Z. Zhou, S. I. El-Hout, J. Yang and J. Zhang, *J. Energy Chem.*, 2021, **54**, 528–554.
- 164 M. V. Galkin and J. S. M. Samec, *ChemSusChem*, 2013, **9**, 1544–1558.
- 165 S. Gazi, *Appl. Catal., B*, 2019, **257**, 117936.
- 166 C. F. Shih, T. Zhang, J. Li and C. Bai, *Joule*, 2018, **2**, 1925–1949.
- 167 N. P. Brandon and Z. Kurban, *Philos. Trans. R. Soc. London, Ser. B*, 2017, **375**, 20160400.
- 168 I. Staffell, D. Scamman, A. V. Abad, P. Balcombe, P. E. Dodds, P. Ekins, N. Shah and K. R. Ward, *Energy Environ. Sci.*, 2019, **12**, 463–491.
- 169 S. Reischauer and B. Pieber, *Isience*, 2021, **24**(3), 102209.
- 170 G. C. de Assis, I. M. A. Silva, T. G. dos Santos, T. V. dos Santos, M. R. Meneghetti and S. M. P. Meneghetti, *Catal. Sci. Technol.*, 2021, **11**, 2354–2360.
- 171 Z. Huang, N. Luo, C. Zhang and F. Wang, *Nat. Rev. Chem*, 2022, **6**, 197–214.
- 172 A. Caravaca, W. Jones, C. Hardacre and M. Bowker, *Phys. Eng. Sci.*, 2016, **472**, 20160054.
- 173 J. Zou, G. Zhang and X. Xu, *Appl. Catal., A*, 2018, **563**, 73–79.
- 174 L. Wang, Z. Zhang, L. Zhang, S. Xue, W. OS Doherty, I. M. O'Hara and X. Ke, *RSC Adv.*, 2015, **104**, 85242–85247.
- 175 W. Liang, R. Zhu, X. Li, J. Deng and Y. Fu, *Green Chem.*, 2021, **23**, 6604–6613.
- 176 L. Zhang, R. Chen, J. Luo, J. Miao, J. Gao and B. Liu, *Nano Res.*, 2016, **9**, 3388–3393.
- 177 X. Lu, S. Xie, H. Yang, Y. Tong and H. Ji, *Chem. Soc. Rev.*, 2014, **43**, 7581–7593.
- 178 G. Iervolino, V. Vaiano, D. Sannino, L. Rizzo, A. Galluzzi, M. Polichetti, G. Pepe and P. Campiglia, *Int. J. Hydrogen Energy*, 2018, **43**, 2184–2196.
- 179 H. F. Ye, R. Shi, X. Yang, W. F. Fu and Y. Chen, *Appl. Catal., B*, 2018, **223**, 70–79.
- 180 G. Kumari, X. Zhang, D. Devasia, J. Heo and P. K. Jain, *ACS Nano*, 2018, **12**, 8330–8340.
- 181 M. M. Hasan, G. E. Khedr and N. K. Allam, *ACS Appl. Nano Mater.*, 2022, **5**, 15457–15464.
- 182 I. M. Badawy, G. E. Khedr, A. M. Hafez, E. A. Ashour and N. Allam, *Chem. Commun.*, 2023, **59**, 7974–7977.
- 183 F. Sastre, C. Versluis, N. Meulendijks, J. Rodriguez-Fernandez, J. Sweelssen, K. Elen, M. K. V. Bael, T. den Hartog, M. A. Verheijen and P. Buskens, *ACS Omega*, 2019, **4**, 7369–7377.
- 184 L. Zhang, W. Wang, S. Zeng, Y. Su and H. Hao, *Green Chem.*, 2018, **20**, 3008–3013.



- 185 B. Ohtani, *Phys. Chem. Chem. Phys.*, 2014, **16**, 1788–1797.
- 186 L. Hu, L. Lin, Z. Wu, S. Zhou and S. Liu, *Renewable Sustainable Energy Rev.*, 2017, **74**, 230–257.
- 187 M. Mazarji, M. Alvarado-Morales, P. Tsapekos, G. Nabi-Bidhendi, N. M. Mahmoodi and I. Angelidaki, *Environ. Int.*, 2019, **115**, 172–183.
- 188 M. Yan, J. C. Lo, J. T. Edwards and P. S. Baran, *J. Am. Chem. Soc.*, 2016, **138**, 12692–12714.
- 189 F. Collin, *Int. J. Mol. Sci.*, 2019, **20**, 2407.
- 190 R. Verma, R. Belgamwar and V. Polshettiwar, *ACS Mater. Lett.*, 2021, **3**, 574–598.
- 191 Y. Guo and J. Chen, *RSC Adv.*, 2016, **6**, 101968–101973.

